Oncogene (2012) 1-6

www.nature.com/onc

SHORT COMMUNICATION

YAP induces malignant mesothelioma cell proliferation by upregulating transcription of cell cycle-promoting genes

T Mizuno[1,2], H Murakami[1], M Fujii[1], F Ishiguro[1,2], I Tanaka[1], Y Kondo[1], S Akatsuka[3], S Toyokuni[3], K Yokoi[2], H Osada[1,4] and Y Sekido[1,4]

Malignant mesothelioma (MM) shows frequent inactivation of the *neurofibromatosis type 2* (*NF2*) –tumor-suppressor gene. Recent studies have documented that the Hippo signaling pathway, a downstream cascade of Merlin (a product of *NF2*), has a key role in organ size control and carcinogenesis by regulating cell proliferation and apoptosis. We previously reported that MMs show overexpression of *Yes-associated protein* (YAP) transcriptional coactivator, the main downstream effector of the Hippo signaling pathway, which results from the inactivation of *NF2*, *LATS2* and/or *SAV1 genes* (the latter two encoding core components of the mammalian Hippo pathway) or amplification of *YAP* itself. However, the detailed roles of YAP remain unclear, especially the target genes of YAP that enhance MM cell growth and survival. Here, we demonstrated that YAP-knockdown inhibited cell motility, invasion and anchorage-independent growth as well as cell proliferation of MM cells *in vitro*. We analyzed genes commonly regulated by YAP in three MM cell lines with constitutive YAP-activation, and found that the major subsets of YAP-upregulating genes encode cell cycle regulators. Among them, YAP directly induced the transcription of *CCND1* and *FOXM1*, in cooperation with TEAD transcription factor. We also found that knockdown of *CCND1* and *FOXM1* suppressed MM cell proliferation, although the inhibitory effects were less evident than those of YAP knockdown. These results indicate that constitutive YAP activation in MM cells promotes cell cycle progression giving more aggressive phenotypes to MM cells.

Oncogene advance online publication, 30 January 2012; doi:10.1038/onc.2012.5

Keywords: malignant mesothelioma; Hippo pathway; YAP; CCND1; cell cycle

INTRODUCTION

Malignant mesothelioma (MM) is one of the most aggressive neoplasms, which is caused by asbestos exposure.[1,2] It is usually resistant to conventional therapies, and the prognosis of patients is very poor. The median survival of malignant pleural mesothelioma patients after diagnosis is 7–11 months.[1,3,4] There is a 30–40 year interval before clinical presentation of the tumor after asbestos exposure.[5] While the long latency of the disease implies that multiple genetic and epigenetic alterations might be required for MM progression,[6] the detailed molecular pathogenesis of MM has not been well understood.

Among the limited number of genes that are frequently mutated in MMs, inactivation of $p16^{INK4a}/p14^{ARF}$ is detected in over 70% of MMs.[7] The *NF2* gene, which is responsible for the *NF2* familial cancer syndrome, has been shown to be inactivated in 40–50% of MMs.[8,9] A recent study has also indicated that 23% of MM cases had an inactivating mutation of *BAP1*, which encodes a nuclear deubiquitinase.[10,11]

The *NF2* gene encodes Merlin, which is a membrane-cytoskeleton-associated protein with four-point-one, ezrin, radixin and moesin domain, and acts as a tumor suppressor.[12] One of the downstream signaling cascades regulated by Merlin is the Hippo signaling pathway, which is conserved from *Drosophila* to mammalians.[13–15] In MM cells, besides the *NF2* mutation, genetic alterations in the components of the Hippo signaling pathway have also been identified recently, including inactivating mutations of *large tumor suppressor 1* (*LATS1*), *LATS2* and *SAV1*, and amplification of *Yes-associated protein* (*YAP*).[10,16,17] Together with *NF2* mutation, MM shows frequent Merlin-Hippo pathway inactivation, which leads to YAP activation in over 70% of MM cases.[18]

Studies have shown that the Hippo signaling pathway is involved in the cell cycle regulation and the control of organ size.[19,20] The dysregulation of this pathway, which leads to constitutive YAP activation, induces the oncogenic transformation in cooperation with distinct transcription factors such as TEAD family members.[21–24] Overexpression, especially dominant expression in the nuclei compared with the cytoplasm of tumor cells and the oncogenic roles of YAP have been shown in various types of human malignancies.[25–29] On the other hand, the anti-proliferative or apoptosis-inducing function of YAP has also been demonstrated in the context of DNA damage or cellular stress, which induces its binding of YAP with other transcription factors such as p73, a paralog of p53 tumor suppressor.[30–32]

We previously showed that YAP promoted cell proliferation[17] and exogenous LATS2 inhibited cell proliferation via induction of YAP phosphorylation in MM cells.[16] However, the detailed characteristics of YAP oncogenic properties remain unclear, including the exact target genes that are inducible by YAP activation in MM cells. In this study, we aimed to identify the target genes of YAP in MM cells to elaborate how YAP induces the MM-cell malignant phenotypes. We found that cell cycle-regulating genes, including *CCDN1* and *FOXM1*, are induced by YAP, suggesting that the dysregulation of cell cycle regulation is one of the key alterations in which MM cells acquire malignancy by YAP activation.

[1]Division of Molecular Oncology, Aichi Cancer Center Research Institute, Nagoya, Japan; [2]Department of Thoracic Surgery, Nagoya University Graduate School of Medicine, Nagoya, Japan; [3]Department of Pathology and Biological Responses, Nagoya University Graduate School of Medicine, Nagoya, Japan and [4]Department of Cancer Genetics, Program in Function Construction Medicine, Nagoya University Graduate School of Medicine, Nagoya, Japan. Correspondence: Dr Y Sekido, Division of Molecular Oncology, Aichi Cancer Center Research Institute, Kanokoden 1-1, Chikusa-ku, Nagoya, Aichi 464-8681, Japan. E-mail: ysekido@aichi-cc.jp
Received 3 September 2011; revised 19 December 2011; accepted 30 December 2011

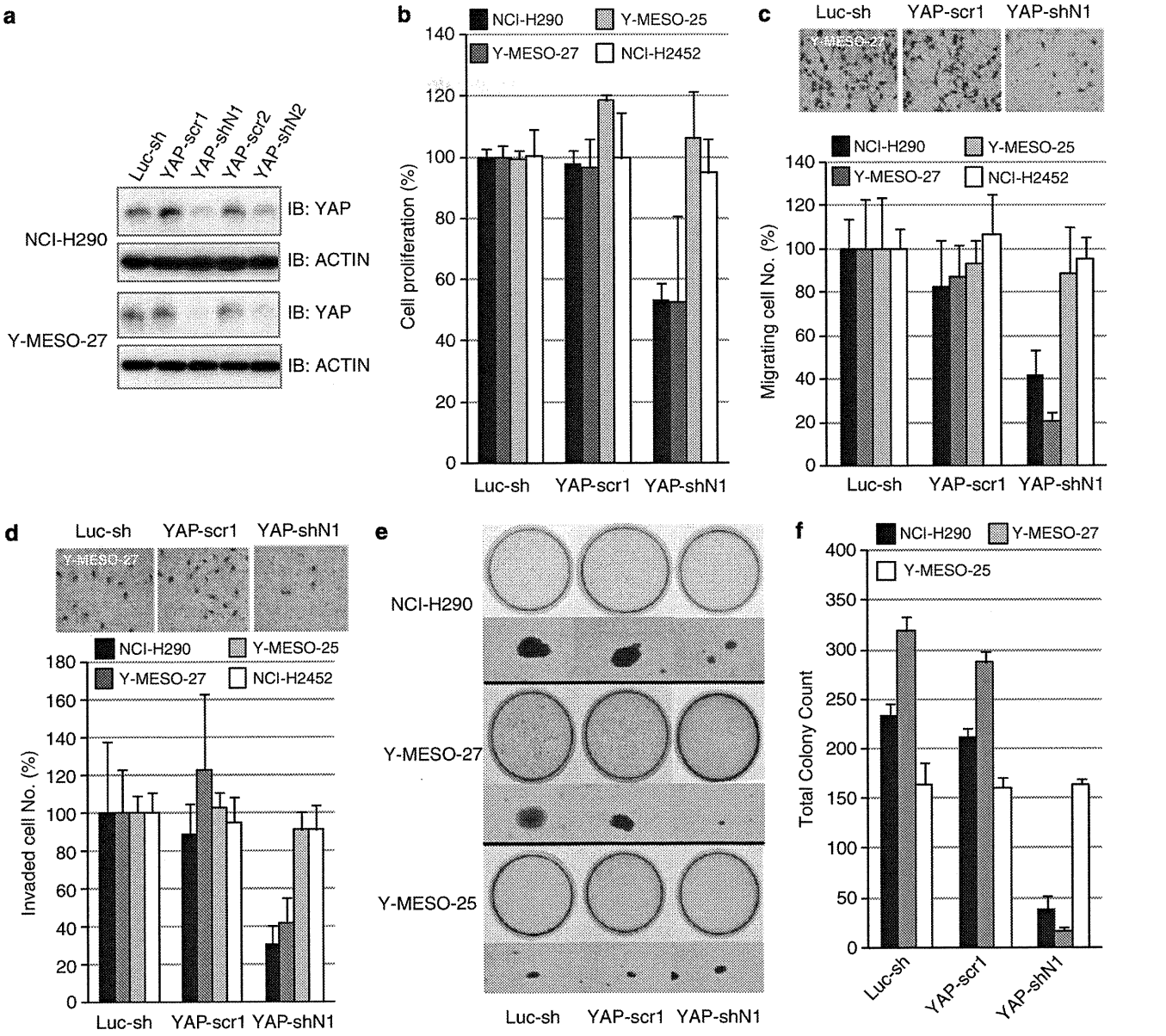

Figure 1. YAP knockdown suppressed malignant phenotypes of MM cell lines with YAP activation (NCI-H290 and Y-MESO-27) but not of those without YAP activation (Y-MESO-25 and NCI-H2452). (**a**) Western blot analyses for knockdown efficacies of short hairpin (sh)-YAP RNA interference lentivirus vectors. Two sh-YAP RNA interference lentivirus vectors (YAP-shN1 and YAP-shN2) contained each target sequence of YAP. Control shRNA vectors for luciferase (Luc-sh) with the target sequence for luciferase and for YAP (YAP-scr1 and YAP-scr2) with each scrambled target sequence were also constructed. Total cell lysates were subjected to western blot analysis using rabbit anti-YAP antibody and mouse anti-β-actin antibody. YAP-shN1 induced more potent YAP suppression compared with YAP-shN2. (**b**) Cell proliferation assay. After 72 h of lentivirus infection, calorimetric assays were performed with Tetra Color One (Seikagaku, Tokyo, Japan) and absorbance was measured at 450 nm. Cell proliferations were reduced to approximately 50% with YAP knockdown in NCI-H290 and Y-MESO-27 cell lines. (**c**) Migration assay. Cell migration and invasion potential were measured by *in vitro* Boyden chamber assays (BD Biosciences Discovery Labware, Bedford, MA, USA). Upper photographs show representative images of the migrating Y-MESO-27 cells. (**d**) Invasion assay. Matrigel matrix insert membrane was used for invasion assay. Upper photographs show representative images of invading Y-MESO-27 cells. (**e**) Soft agar colony formation assays. After a 10 day-incubation, colonies were stained with 0.3% crystal violet. Photographs of low (top) and high magnification (bottom) show that anchorage-independent growth was significantly suppressed with YAP knockdown in NCI-H290 and Y-MESO-27 but not Y-MESO-25 cell line. (**f**) A graphic presentation of the soft agar colony formation assays of (**e**). Columns are the means of experiments, and bars represent s.d. (**b**, **c**, **d**, **f**).

RESULTS AND DISCUSSION

Knockdown of YAP suppressed oncogenic properties of MM cells

We previously reported that several MM cell lines with *NF2* and/or *LATS2* mutations have constitutive YAP activation with low-level phosphorylation of YAP (S127).[16] Using western blot analysis with a panel of 23 MM cell lines, we confirmed that 16 (70%) cell lines showed lower levels of pYAP-S127 than MeT-5A, a transformed normal mesothelial cell line (Supplementary Figure 1). Among them, we selected three MM cell lines with constitutive YAP activation for further analyses; NCI-H290 with *NF2* inactivation, and Y-MESO-27 and Y-MESO-30 with *LATS2* inactivation.

Table 1. Gene ontology and pathway analyses in 228 genes commonly downregulated by YAP knockdown

Rank	*Name*	*Score*	*Score (p)*	*Score (v)*	*Score (c)*
(a) *Top 10 Gene ontology*					
1	Cell cycle (GO:0007049)	137.598	3.791E−042	0.409	0.079
2	Cell cycle process (GO:0022402)	129.250	1.235E−039	0.358	0.090
3	Cell cycle phase (GO:0022403)	117.627	3.897E−036	0.302	0.105
4	Mitotic cell cycle (GO:0000278)	107.258	5.153E−033	0.289	0.097
5	Mitotic phase (GO:0000279)	90.202	7.021E−028	0.214	0.124
6	Regulation of cell cycle (GO:0051726)	86.379	9.939E−027	0.264	0.080
7	Organelle organization (GO:0006996)	82.447	1.517E−025	0.371	0.047
8	Regulation of cell cycle process (GO:0010564)	80.848	4.596E−025	0.176	0.147
9	Regulation of metabolic process (GO:0019222)	76.863	7.275E−024	0.528	0.029
10	Regulation of cellular metabolic process (GO:0031323)	71.798	2.435E−022	0.491	0.030
(b) *Top 10 gene pathway*					
1	Transcriptional regulation by RB/E2F	297.728	2.371E−090	0.234	0.207
2	Transcriptional regulation by FOXM	63.604	7.135E−020	0.043	0.360
3	Aurora signaling pathway	52.246	1.872E−016	0.038	0.258
4	CDK signaling pathway	46.256	1.190E−014	0.043	0.107
5	PLK signaling pathway	45.168	2.531E−014	0.033	0.241
6	Transcriptional regulation by AP-1	35.712	1.777E−011	0.038	0.067
7	Nucleophosmin signaling pathway	29.087	1.753E−009	0.024	0.152
8	Wnt signaling pathway	28.376	2.870E−009	0.029	0.076
9	Transcriptional regulation by Myb	27.041	7.242E−009	0.029	0.065
10	PIN1 signaling pathway	22.329	1.898E−007	0.024	0.061

Abbreviations: AP-1, adaptor-related protein complex 1; CDK, cyclin-dependent kinase; FOXM, forkhead box M; Myb, v-myb myeloblastosis viral oncogene homolog; PIN, peptidylprolyl cis/trans isomerase NIMA-interacting 1; PLK, polo-like kinase; RB/E2F, retinoblastoma/E2F transcription factor.

As we previously showed that YAP inhibition suppressed NCI-H290 cell proliferation,[17] we first confirmed that a newly established YAP-shRNA lentivirus more efficiently suppressed the YAP expression and inhibited the cell proliferation of NCI-H290 cell line and another MM cell line, Y-MESO-27, which had *LATS2* deletion, but not in two other MM cell lines, Y-MESO-25 and NCI-H2452, without YAP activation (Figures 1a and b). Next, we analysed whether YAP knockdown affected other malignant phenotypes of MM cells *in vitro*. Both motility and invasive abilities were significantly inhibited in NCI-H290 and Y-MESO-27 cells (Figures 1c and d). Anchorage-independent growth analysis revealed a nearly complete suppression of colony formation in Y-MESO-27 cells and an 80% decrease in NCI-H290 cells (Figures 1e and f). These results indicate that YAP suppression in MM cells with constitutively activated YAP induces significant suppression of motility, invasion and anchorage-independent growth as well as cell proliferation *in vitro*.

Identification of YAP-regulating genes by microarray-based expression profiling analysis

As for the target genes of YAP orthologs, *cyclin E, Diap1* and *bantam* microRNA have been identified for *Drosophila Yokie*.[19] For mammalian YAP, although several genes including the *connective tissue growth factor* (*CTGF*) gene were shown as direct target genes of YAP,[24] other possible candidate target genes for mammalian counterparts do not seem to be really substantiated yet or even excluded, implying that YAP target genes vary among different species as well as among different cell types.

To identify the genes inducible for expression by YAP and responsible for MM cell proliferation, we performed microarray-based expression profiling analysis of the three MM cell lines after YAP knockdown. We found that 1381, 650 and 2097 genes were downregulated to equal or less than 0.5 in the NCI-H290, Y-MESO-27 and Y-MESO-30 cells, respectively, compared with each counterpart cell with the control vector (data not shown). We found that 228 genes were commonly downregulated by YAP knockdown, suggesting that this gene set includes strong candidates for YAP target genes in MM cells (Supplementary Table 1). To characterize the 228 genes, we performed gene ontology analysis and found that the large portion of YAP-regulatory genes is associated with cell cycle regulation (Table 1). Subsequent pathway analysis revealed that the pathways of transcriptional regulation by *RB/E2F* and *FOXM* were most significantly correlated (Table 1).

Meanwhile, our results revealed that 156 genes were commonly upregulated after YAP knockdown over twofold (Supplementary Table 1). Gene ontology and pathway analyses indicated that genes involved in wounding, inflammation and cell–extracellular matrix adhesion were upregulated, suggesting that suppression of these signaling pathways might also contribute to malignant phenotypes of MM cells by YAP activation, albeit their expressions might be indirectly suppressed (Supplementary Table 2).

YAP regulates CCND1 and FOXM1 transcription directly in cooperation with TEAD

Among the identified cell cycle regulatory genes, we focused on *CCND1*, a G1 cyclin-regulating RB/E2F pathway, and *FOXM1*, a transcription factor targeting both G1/S and G2/M progression regulators. *CCND1* and *FOXM1* were found to be commonly downregulated in the three cell lines from 0.13 to 0.48 and from 0.13- to 0.42-changes, respectively (Supplementary Table 1). Moreover, their promoter regions were also likely to harbor a putative recognition motif of TEAD, a transcriptional factor that binds to YAP.

To determine whether YAP regulates transcription of *CCND1* and *FOXM1* directly in MM cells, we carried out a chromatin immunoprecipitation assay. We prepared a primer set for the proximal promoter region of both genes to include the putative TEAD recognition motif[33] (Figure 2a). When precipitated with anti-YAP antibody, we detected positive PCR products of the proximal promoter regions of both genes, which indicated the direct binding of YAP to the *CCND1* and *FOXM1* proximal promoter regions (Figure 2b), although they were not detected in the distal regions (data not shown).

Next, to determine whether YAP induces transcription of *CCND1* and *FOXM1*, and then transcription is further enhanced

by exogenous TEAD transcription factor, we performed luciferase reporter assay for the promoter regions of these genes (Figure 2a) with YAP wild type and its constitutively active form, YAP S127A. We found that cotransduction of wild-type TEAD4 with YAP wild type or the active mutant form significantly induced both *CCND1* and *FOXM1* promoter activities. On the other hand, cotransduction of other mutant forms including YAP S94A[24] or TEAD4ΔCt,[34] both of which were thought to disrupt the YAP-TEAD interaction, did not show the enhancement of luciferase activity (Figures 2c and d).

These results provided support for the notion that *CCND1* and *FOXM1* might be the direct target genes of YAP in MM cells. Consistent with our observations, induction of *CCND1* by YAP has also been suggested by other studies. For example, in vertebrate neural tube development, YAP and TEAD promoted cell cycle progression by inducing *CCND1*.[21] As an upstream suppressive regulator of YAP, Merlin was also shown to inhibit *CCND1* expression by using *NF2*-deficient MM cells.[35] Although those reports did not refer to transcriptional regulation of *CCND1* by YAP, they demonstrated a contribution of Hippo signaling pathway to *CCND1* regulation, which our present findings corroborate.

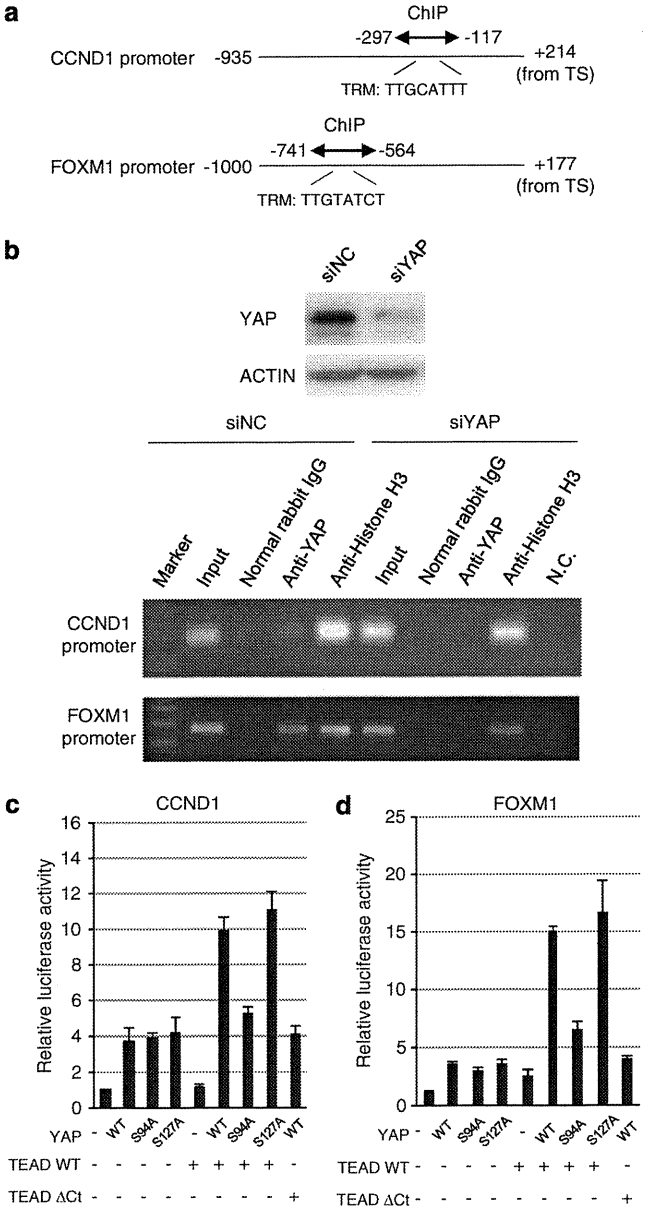

Figure 2. YAP directly induces transcription of the *CCND1* and *FOXM1* genes. (**a**) Each promoter includes the putative TEAD recognition motif (TRM), XDGHATXT, where X = A, T, C or G; D = A or T; and H = A, T or C. ChIP primer sets (arrow) were designed to include the motif. DNA fragments of nucleotide position −935 to +214 for *CCND1* and nucleotide position −1000 to +177 for *FOXM1* were inserted into luciferase reporter vectors. TS: transcriptional start. (**b**) ChIP assay using ChIP kit (ab500, Abcam) demonstrated that YAP bound to the *CCND1* and *FOXM1* proximal promoter regions. NCI-H290 cells treated with YAP siRNA (siYAP; Ambion, Austin, TX) were used as YAP-suppressed control, while cells with an irrelevant siRNA (siNC) maintained high YAP expression, as confirmed with western blot analysis. (Upper panel) After the cells with high or low YAP expression were subjected to immunoprecipitation assay with normal rabbit IgG (SC2027, Santa Cruz), rabbit anti-YAP antibody, or anti-H3 antibody (ab1791, Abcam) and protein A beads, immunoprecipitated chromatin were decross-linked. Recruited DNA was subjected to PCR using primer sets for proximal promoter regions of *CCND1* and *FOXM1*, and PCR products were electrophoresed in agarose gel. (Lower panel) Note that amounts of PCR products from the chromatin, which was precipitated with the anti-YAP antibody, were suppressed by pretreatment with siYAP. (**c, d**) For reporter assay, MeT-5A cells were transfected with the pGL3 basic firefly luciferase reporter plasmid with the *CCND1* or *FOXM1* promoter region by using FuGENE 6 transfection reagent (Roche, Mannheim, Germany). Renilla luciferase plasmid was also transfected for internal control. Thirty-six hours later, cells were lysed and subjected to dual-luciferase assay (TOYO INK, Tokyo, Japan). The promoter activities were enhanced with combined transduction of TEAD4 WT with wild type (WT) or constitutively activated forms of YAP (YAP S127A), but not with YAP S94A (inactive for TEAD binding) or TEAD4ΔCt (inactive for YAP binding) forms. Columns are the means of experiments, and bars represent s.d. (**c, d**).

YAP depletion suppressed cell cycle-promoting gene expressions in MM cells

The gene ontology analysis based on the microarray-based expression profiling suggested a significant contribution of YAP to the cell cycle process in MM cells. Based on our previous data indicating G1 cell cycle arrest in NCI-H290 cells by YAP knockdown,[17] we studied the status of cell cycle and expressions of cell cycle-promoting genes in a time-dependent manner after YAP-shRNA lentivirus infection. We found that G1 cell cycle arrest occurred at as early as 48 h, and the population of G1 cell cycle arrest increased at 72 h (Figure 3a). With quantitative real-time RT-PCR analysis, suppression of the *CCND1* gene expression was revealed to follow the downregulation of *YAP* as expected (Figure 3c). Consistent with the expression array analysis, other cell cycle-promoting genes including *E2F1, Aurora kinase B* (*AURKB*), *Polo-like kinase 1* (*PLK1*) and *NIMA-related kinase 2* (*NEK2*), also showed the decrease in the expression levels according to YAP-downregulation (Figure 3c). However, other irrelevant genes such as *SMAD3* did not show any decrease (data not shown). These results suggested that, together with YAP-direct target genes of *CCND1* and *FOXM1*, other cell-promoting genes are also involved in the dysregulated cell cycle machinery in YAP-activated MM cells.

Additionally, we observed that YAP-knockdown increased subG1 population of the cells in flow cytometric analysis (Figure 3b) and affected the expression levels of several apoptotic-related genes, including the downregulation of *BIRC5* (also known as *survivin*), an anti-apoptotic gene, and upregulated the one of *BCL2L11* (also known as *BIM*), a pro-apoptotic gene (Supplementary Table 2). In a flow cytometric assay with

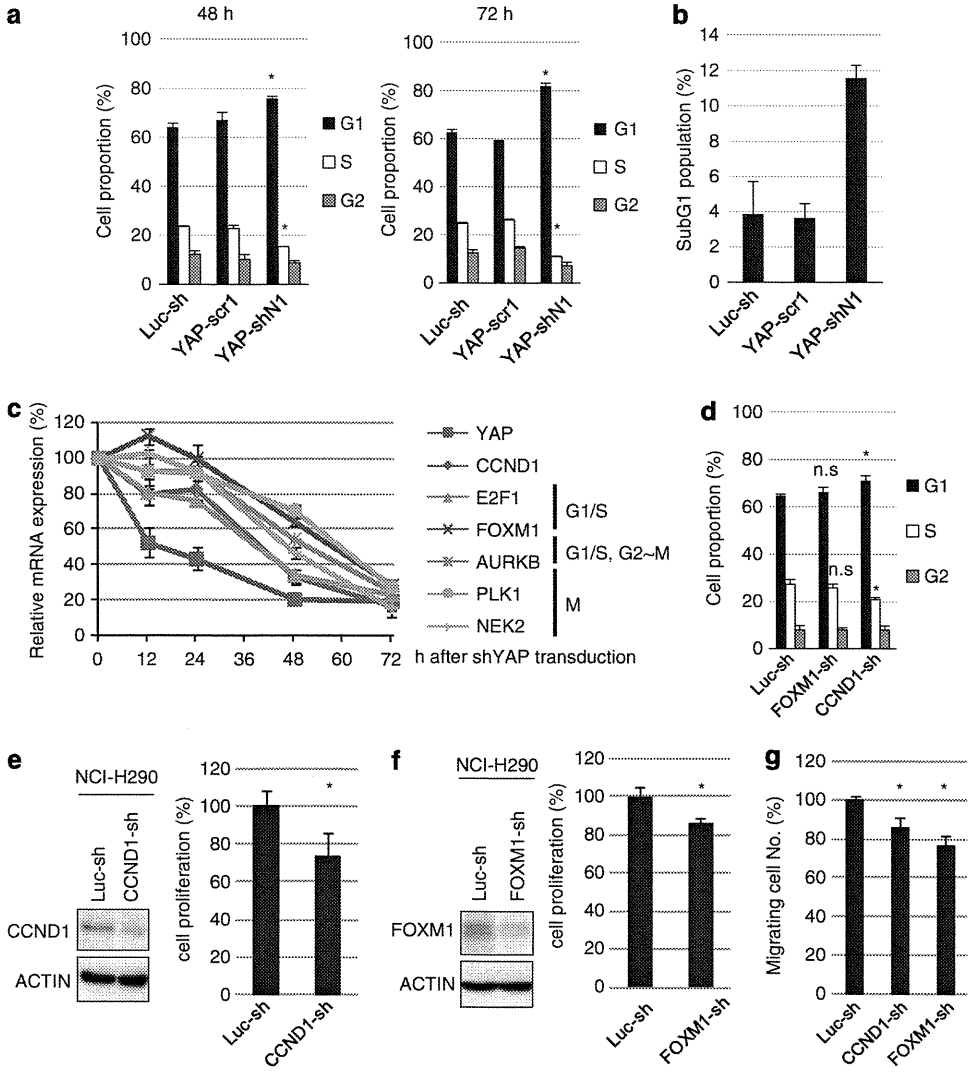

Figure 3. Involvement of YAP, CCND1 and FOXM1 in cell proliferation in NCI-H290 cells. (**a**) Flow cytometry analysis. After infection with YAP-shN1, YAP-scr1, or Luc-sh lentivirus, cells were incubated to grow for 48 or 72 h. Cells were harvested, washed with PBS and fixed with 70% ethanol. After treatment by RNaseA, cells were stained with propidium iodide (Sigma) and flow cytometry analysis was carried out. Cell cycle analysis revealed increased population of G1 phase and decreased population of S phase in NCI-H290 cells 48 h (left) and 72 h (right), respectively, after YAP-shN1 lentivirus infection. (**b**) YAP-knockdown induced subG1 population of MM cells. (**c**) Quantitative real-time RT-PCR analysis was performed with ABI 7500 Real-Time PCR System (Applied Biosystems, Foster, CA, USA). Glyceraldehyde-3-phosphate dehydrogenase (GAPDH) served as an endogenous control. The graph shows the changes in mRNA expression levels of cell cycle-related genes in response to YAP depletion. Symbols are the means of experiments normalized to control cell, and bars represent s.d. (**d**) Flow cytometry analysis. Knockdown of *CCND1* modestly increased the number of G1/S arrest cells in MM cells. (**e**, **f**) Cell proliferation assay. Knockdown of *CCND1* (**e**) and *FOXM1* (**f**) moderately suppressed cell proliferation in NCI-H290 cells. (**g**) Cell migration assay. Knockdown of *CCND1* and *FOXM1* induced modest suppression of NCI-H290 cell migratory activity. Columns are the means of experiments, and bars represent s.d. Asterisks represent $P<0.05$ between YAP-shN1 (**a**), CCND1-sh (**d**, **e**, **g**), or FOXM1-sh (**d**, **f**, **g**) versus Luc-sh control. n.s., not significant.

annexin V, a modest increase of early apoptotic cell population was also detected (Supplementary Figure 2). Although these data suggested apoptosis induction in MM cells, we did not find significant caspase activation with western blot analysis probably due to a relatively small population of MM cells that underwent apoptosis (data not shown). Thus, further studies may be warranted to clarify the underlying mechanism and significance of cell death by YAP-knockdown in MM cells.

CCND1 contributes to G1/S transition in MM cells

To determine whether knockdown of individual cell cycle specific genes regulated by YAP is sufficient to induce G1 cell cycle arrest in MM cells, we performed cell cycle analysis of NCI-H290 cells with knockdown of *CCND1* or *FOXM1*. After transduction of CCND1-sh, we found that the cell population of G1 phase increased and that of S phase decreased compared with the control cell (Figure 3d), although the effect was weaker than that of YAP-sh. However, the effect of FOXM1-sh on cell cycle progression was not clear (Figure 3d).

Finally, to evaluate proliferative roles of CCND1 or FOXM1 as YAP transcriptional targets in MM cells, we knocked down *CCND1* and *FOXM1* and performed proliferation analysis. The depletion of CCND1 and FOXM1 caused modest suppression compared with YAP depletion, though the decrease of proliferation was larger in CCND1 depletion than FOXM1 depletion at 26% and 14%,

respectively (Figures 3e and f). Taken together, these results suggested that YAP contributes to expression of a wide range of cell cycle-promoting genes and induces MM cell proliferation, although knockdown of individual YAP target genes shows moderate effects.

In conclusion, we showed that YAP induces multiple gene expression, which includes cell cycle-promoting genes such as *CCND1* and *FOXM1* in MM cells. Our findings thus serve to elucidate some important aspects of dysregulated cell cycle control mechanisms in MM cells through YAP activation. As individual inhibition of YAP target genes did not suppress MM proliferation sufficiently, we speculate that a wide range of genes evoked by YAP activation induce MM cell proliferation and progression as a whole. Thus, our results suggest that YAP itself may be a key target molecule for the development of a new molecular target therapy for MM.

CONFLICT OF INTEREST

The authors declare no conflict of interest.

ACKNOWLEDGEMENTS

We thank Ms Mika Yamamoto for her excellent technical assistance. This work was supported in part by a Special Coordination Fund for Promoting Science and Technology from the Ministry of Education, Culture, Sports, Science and Technology of Japan (H18-1-3-3-1), KAKENHI (18390245, 22300338), Grant-in-Aid for Third-Term Comprehensive Control Research for Cancer from the Ministry of Health, Labor and Welfare of Japan, the Takeda Science Foundation and the Kobayashi Foundation for Cancer Research.

REFERENCES

1 Pass HI, Vogelzang N, Hahn S, Carbone M. Malignant pleural mesothelioma. *Curr Probl Cancer* 2004; **28**: 93-174.
2 Yang H, Testa JR, Carbone M. Mesothelioma epidemiology, carcinogenesis, and pathogenesis. *Curr Treat Options Oncol* 2008; **9**: 147-157.
3 Robinson BW, Lake RA. Advances in malignant mesothelioma. *N Engl J Med* 2005; **353**: 1591-1603.
4 Vogelzang NJ, Rusthoven JJ, Symanowski J, Denham C, Kaukel E, Ruffie P *et al.* Phase III study of pemetrexed in combination with cisplatin versus cisplatin alone in patients with malignant pleural mesothelioma. *J Clin Oncol* 2003; **21**: 2636-2644.
5 Carbone M, Kratzke RA, Testa JR. The pathogenesis of mesothelioma. *Semin Oncol* 2002; **29**: 2-17.
6 Sekido Y. Genomic abnormalities and signal transduction dysregulation in malignant mesothelioma cells. *Cancer Sci* 2010; **101**: 1-6.
7 Illei PB, Ladanyi M, Rusch VW, Zakowski MF. The use of CDKN2A deletion as a diagnostic marker for malignant mesothelioma in body cavity effusions. *Cancer* 2003; **99**: 51-56.
8 Bianchi AB, Mitsunaga SI, Cheng JQ, Klein WM, Jhanwar SC, Seizinger B *et al.* High frequency of inactivating mutations in the neurofibromatosis type 2 gene (NF2) in primary malignant mesotheliomas. *Proc Natl Acad Sci USA* 1995; **92**: 10854-10858.
9 Sekido Y, Pass HI, Bader S, Mew DJ, Christman MF, Gazdar AF *et al.* Neurofibromatosis type 2 (NF2) gene is somatically mutated in mesothelioma but not in lung cancer. *Cancer Res* 1995; **55**: 1227-1231.
10 Bott M, Brevet M, Taylor BS, Shimizu S, Ito T, Wang L *et al.* The nuclear deubiquitinase BAP1 is commonly inactivated by somatic mutations and 3p21.1 losses in malignant pleural mesothelioma. *Nat Genet* 2011; **43**: 668-672.
11 Testa JR, Cheung M, Pei J, Below JE, Tan Y, Sementino E *et al.* Germline BAP1 mutations predispose to malignant mesothelioma. *Nat Genet* 2011; **43**: 1022-1025.
12 Hamaratoglu F, Willecke M, Kango-Singh M, Nolo R, Hyun E, Tao C *et al.* The tumour-suppressor genes NF2/Merlin and expanded act through Hippo signalling to regulate cell proliferation and apoptosis. *Nat Cell Biol* 2006; **8**: 27-36.
13 Dong J, Feldmann G, Huang J, Wu S, Zhang N, Comerford SA *et al.* Elucidation of a universal size-control mechanism in Drosophila and mammals. *Cell* 2007; **130**: 1120-1133.
14 Saucedo LJ, Edgar BA. Filling out the Hippo pathway. *Nat Rev Mol Cell Biol* 2007; **8**: 613-621.
15 Zhang N, Bai H, David KK, Dong J, Zheng Y, Cai J *et al.* The Merlin/NF2 tumor suppressor functions through the YAP oncoprotein to regulate tissue homeostasis in mammals. *Dev Cell* 2010; **19**: 27-38.
16 Murakami H, Mizuno T, Taniguchi T, Fujii M, Ishiguro F, Fukui T *et al.* LATS2 is a tumor suppressor gene of malignant mesothelioma. *Cancer Res* 2011; **71**: 873-883.
17 Yokoyama T, Osada H, Murakami H, Tatematsu Y, Taniguchi T, Kondo Y *et al.* YAP1 is involved in mesothelioma development and negatively regulated by Merlin through phosphorylation. *Carcinogenesis* 2008; **29**: 2139-2146.
18 Sekido Y. Inactivation of Merlin in malignant mesothelioma cells and the Hippo signaling cascade dysregulation. *Pathol Int* 2011; **61**: 331-344.
19 Huang J, Wu S, Barrera J, Matthews K, Pan D. The Hippo signaling pathway coordinately regulates cell proliferation and apoptosis by inactivating Yorkie, the Drosophila homolog of YAP. *Cell* 2005; **122**: 421-434.
20 Tapon N, Harvey KF, Bell DW, Wahrer DC, Schiripo TA, Haber DA *et al.* Salvador promotes both cell cycle exit and apoptosis in Drosophila and is mutated in human cancer cell lines. *Cell* 2002; **110**: 467-478.
21 Cao X, Pfaff SL, Gage FH. YAP regulates neural progenitor cell number via the TEA domain transcription factor. *Genes Dev* 2008; **22**: 3320-3334.
22 Nishioka N, Inoue K, Adachi K, Kiyonari H, Ota M, Ralston A *et al.* The Hippo signaling pathway components Lats and Yap pattern Tead4 activity to distinguish mouse trophectoderm from inner cell mass. *Dev Cell* 2009; **16**: 398-410.
23 Zhang X, Milton CC, Humbert PO, Harvey KF. Transcriptional output of the Salvador/Warts/Hippo pathway is controlled in distinct fashions in Drosophila melanogaster and mammalian cell lines. *Cancer Res* 2009; **69**: 6033-6041.
24 Zhao B, Ye X, Yu J, Li L, Li W, Li S *et al.* TEAD mediates YAP-dependent gene induction and growth control. *Genes Dev* 2008; **22**: 1962-1971.
25 Hall CA, Wang R, Miao J, Oliva E, Shen X, Wheeler T *et al.* Hippo pathway effector Yap is an ovarian cancer oncogene. *Cancer Res* 2010; **70**: 8517-8525.
26 Muramatsu T, Imoto I, Matsui T, Kozaki K, Haruki S, Sudol M *et al.* YAP is a candidate oncogene for esophageal squamous cell carcinoma. *Carcinogenesis* 2011; **32**: 389-398.
27 Wang Y, Dong Q, Zhang Q, Li Z, Wang E, Qiu X. Overexpression of yes-associated protein contributes to progression and poor prognosis of non-small-cell lung cancer. *Cancer Sci* 2010; **101**: 1279-1285.
28 Xu MZ, Yao TJ, Lee NP, Ng IO, Chan YT, Zender L *et al.* Yes-associated protein is an independent prognostic marker in hepatocellular carcinoma. *Cancer* 2009; **115**: 4576-4585.
29 Zhang X, George J, Deb S, Degoutin JL, Takano EA, Fox SB *et al.* The Hippo pathway transcriptional co-activator, YAP, is an ovarian cancer oncogene. *Oncogene* 2011; **30**: 2810-2822.
30 Basu S, Totty NF, Irwin MS, Sudol M, Downward J. Akt phosphorylates the Yes-associated protein, YAP, to induce interaction with 14-3-3 and attenuation of p73-mediated apoptosis. *Mol Cell* 2003; **11**: 11-23.
31 Lapi E, Di Agostino S, Donzelli S, Gal H, Domany E, Rechavi G *et al.* PML, YAP, and p73 are components of a proapoptotic autoregulatory feedback loop. *Mol Cell* 2008; **32**: 803-814.
32 Levy D, Adamovich Y, Reuven N, Shaul Y. The Yes-associated protein 1 stabilizes p73 by preventing Itch-mediated ubiquitination of p73. *Cell Death Differ* 2007; **14**: 743-751.
33 Anbanandam A, Albarado DC, Nguyen CT, Halder G, Gao X, Veeraraghavan S. Insights into transcription enhancer factor 1 (TEF-1) activity from the solution structure of the TEA domain. *Proc Natl Acad Sci USA* 2006; **103**: 17225-17230.
34 Vassilev A, Kaneko KJ, Shu H, Zhao Y, DePamphilis ML. TEAD/TEF transcription factors utilize the activation domain of YAP65, a Src/Yes-associated protein localized in the cytoplasm. *Genes Dev* 2001; **15**: 1229-1241.
35 Xiao GH, Gallagher R, Shetler J, Skele K, Altomare DA, Pestell RG *et al.* The NF2 tumor suppressor gene product, merlin, inhibits cell proliferation and cell cycle progression by repressing cyclin D1 expression. *Mol Cell Biol* 2005; **25**: 2384-2394.

Supplementary Information accompanies the paper on the Oncogene website (http://www.nature.com/onc)

G Model
LUNG-3966; No. of Pages 8
ARTICLE IN PRESS

Lung Cancer xxx (2011) xxx–xxx

Contents lists available at SciVerse ScienceDirect

Lung Cancer

journal homepage: www.elsevier.com/locate/lungcan

Conversion from the "oncogene addiction" to "drug addiction" by intensive inhibition of the EGFR and MET in lung cancer with activating *EGFR* mutation

Kenichi Suda[a,c], Kenji Tomizawa[a], Hirotaka Osada[b], Yoshihiko Maehara[c], Yasushi Yatabe[d], Yoshitaka Sekido[b], Tetsuya Mitsudomi[a,*]

[a] *Department of Thoracic Surgery, Aichi Cancer Center Hospital, 1-1 Kanokoden, Chikusa-ku, Nagoya, Japan*
[b] *Division of Molecular Oncology, Aichi Cancer Center Research Institute, 1-1 Kanokoden, Chikusa-ku, Nagoya, Japan*
[c] *Department of Surgery and Science, Graduate School of Medical Science, Kyushu University, 3-1-1 Maidashi, Higashi-ku, Fukuoka, Japan*
[d] *Department of Pathology and Molecular Diagnostics, Aichi Cancer Center Hospital, 1-1 Kanokoden, Chikusa-ku, Nagoya, Japan*

ARTICLE INFO

Article history:
Received 2 September 2011
Received in revised form 25 October 2011
Accepted 5 November 2011

Keywords:
EGFR mutation
Acquired resistance
Tyrosine kinase inhibitors
Molecular target therapy
Irreversible EGFR inhibitor
PTEN

ABSTRACT

Emergence of acquired resistance is virtually inevitable in patients with a mutation in the epidermal growth factor receptor gene (*EGFR*) treated with EGFR tyrosine kinase inhibitors (TKIs). Several novel TKIs that may prevent or overcome the resistance mechanisms are now under clinical development. However, it is unknown how tumor cells will respond to intensive treatment using these novel TKIs. We previously established HCC827EPR cells, which are T790M positive, through combined treatment with erlotinib and a MET-TKI from erlotinib-hypersensitive HCC827 cells. In this study, we treated HCC827EPR cells sequentially with an irreversible EGFR-TKI, CL-387,785, to establish resistant cells (HCC827CLR), and we analyzed the mechanisms responsible for resistance. In HCC827CLR cells, *PTEN* expression was downregulated and Akt phosphorylation persisted in the presence of CL-387,785. Akt inhibition restored CL-387,785 sensitivity. In addition, withdrawal of CL-387,785 reduced cell viability in HCC827CLR cells, indicating that these cells were "addicted" to CL-387,785. HCC827CLR cells overexpressed the EGFR, and inhibition of the EGFR or MEK–ERK was needed to maintain cell proliferation. Increased senescence was observed in HCC827CLR cells in the drug-free condition. Through long-term culture of HCC827CLR cells without CL-387,785, we established HCC827-CL-387,785-independent cells, which exhibited decreased *EGFR* expression and a mesenchymal phenotype. In conclusion, *PTEN* downregulation is a newly identified mechanism underlying the acquired resistance to irreversible EGFR-TKIs after acquisition of T790M against erlotinib. This series of experiments highlights the flexibility of cancer cells that have adapted to environmental stresses induced by intensive treatment with TKIs.

1. Introduction

Epidermal growth factor receptor (*EGFR*)-mutated lung cancers are addicted to mutated EGFR. Patients with lung cancers harboring *EGFR* mutations often dramatically respond to orally available EGFR tyrosine kinase inhibitors (TKIs) [1–3]. However, acquired resistance develops in almost all patients, usually within 1 year, and this limits the improvement in patient outcomes. Therefore, it is essential to develop treatment strategies that can prevent or overcome the emergence of acquired resistance.

The common mechanisms underlying acquired resistance include the T790M *EGFR* secondary mutation and *MET* gene amplification, which are present in about 50% and 5–20% of the tumors with acquired resistance, respectively [4–7]. Because the T790M mutation confers resistance by increasing the affinity of the EGFR for ATP relative to that for TKIs [8], several kinds of irreversible TKIs that covalently bind to cysteine 797 at the catalytic pocket of EGFR are expected to overcome this type of resistance. In addition, several MET-TKIs are also now under clinical development. Intensive treatment using these kinase inhibitors may be applied to clinic in the near future, but at present, it is unknown how tumor cells will respond to such treatment.

HCC827 lung adenocarcinoma cells harbor a deletion mutation in exon 19 of *EGFR* and are very sensitive to EGFR-TKIs. A recent report has revealed the preexistence of minor clones with *MET* amplification (about 0.1%) in HCC827 cells untreated with EGFR-TKIs [9], and this cell line often acquires resistance to EGFR-TKIs through *MET* amplification [6,9,10]. Therefore, we treated HCC827 cells with increasing concentrations of erlotinib in the presence of the MET-TKI, PHA-665,752, and obtained cells resistant to the combination of both drugs; we have designated these HCC827EPR cells. HCC827EPR cells have an acquired EGFR T790M mutation

* Corresponding author. Tel.: +81 52 762 6111; fax: +81 52 764 2963.
E-mail address: mitsudom@aichi-cc.jp (T. Mitsudomi).

0169-5002/$ – see front matter © 2011 Elsevier Ireland Ltd. All rights reserved.
doi:10.1016/j.lungcan.2011.11.007

Please cite this article in press as: Suda K, et al. Conversion from the "oncogene addiction" to "drug addiction" by intensive inhibition of the EGFR and MET in lung cancer with activating *EGFR* mutation. Lung Cancer (2011), doi:10.1016/j.lungcan.2011.11.007

and are sensitive to the irreversible EGFR-TKI, CL-387,785. We decided to establish an *in vitro* model of acquired resistance to CL-387,785 sequentially from HCC827EPR cells with T790M mutation, and investigated the mechanisms responsible for the resistance.

2. Materials and methods

2.1. Cell lines and reagents

The *EGFR* mutant human lung adenocarcinoma cell line HCC827 (del L746_A750) was a kind gift of Dr. Adi F. Gazdar. A subclone of HCC827EPR cells (HCC827EPR.S10 cells) was developed previously in our laboratory [10]. HCC827EPR.S10 cells harbor the T790M mutation in addition to the exon 19 deletion mutation in the *EGFR* gene. These cells were cultured in RPMI-1640 medium supplemented with 5% FBS and 1× antibiotic–antimycotic solution (Invitrogen, Carlsbad, CA) at 37 °C in a humidified incubator with 5% CO_2.

Erlotinib was kindly provided by Hoffmann-La Roche Inc. (Nutley, NJ). CL-387,785 was purchased from Calbiochem (San Diego, CA). PHA-665,752 was purchased from Tocris Bioscience (Ellisville, MO). Two kinds of MEK inhibitor (PD0325901 and AZD6244) and an AKT 1/2 Kinase Inhibitor were purchased from Wako (Osaka, Japan).

2.2. Generation of in vitro CL-387,785-resistant cells

CL-387,785-resistant HCC827 (HCC827CLR) cells were developed from HCC827EPR.S10 cells through the chronic, repeated exposure to increasing concentrations of CL-387,785 from 100 nM to 1 μM, as described previously [6]. CL-387,785-free HCC827 (HCC827CLF) cells were developed from HCC827CLR cells by culturing cells without any drugs for 1 month.

Cell proliferation was measured using TetraColor ONE (Seikagaku-kogyo, Tokyo, Japan), according to the manufacturer's instructions [10]. Parental or resistant cells were incubated for 24 h and then an additional 72 h with drug(s) at the concentrations indicated, and cell growth was assessed.

2.3. Mutation, gene copy number, and expression analyses

Genomic DNA was extracted using a FastPure DNA Kit (Takara Bio, Otsu, Japan). Total RNA was prepared using a mirVana miRNA Isolation Kit (Qiagen, Valencia, CA). Random-primed, first-strand cDNA was synthesized from total RNA using Superscript II (Invitrogen), according to the manufacturer's instructions.

Mutation analysis of exons 18–21 of the *EGFR* gene was performed via direct sequencing after one-step reverse transcription PCR (RT-PCR) from total RNA using the Qiagen OneStep Reverse Transcription PCR Kit (Qiagen), as reported previously [11].

The numbers of copies of the *MET* gene and the *EGFR* gene relative to a *LINE-1* repetitive element were measured using quantitative real-time PCR using the SYBR Green Method (Power SYBR Green PCR Master Mix; Qiagen) on an ABI PRISM 7900HT Sequence Detection System (Applied Biosystems, Foster City, CA) as described previously [6,12]. Normal genomic DNA was used as a standard sample.

Quantitative real-time RT-PCR was performed on first-strand cDNA using TaqMan probes and the TaqMan Universal PCR Master Mix (Applied Biosystems). TaqMan probes for *EGFR* and *PTEN* were purchased from Applied Biosystems and the amplification was performed on an ABI PRISM 7900HT Sequence Detection System (Applied Biosystems). Quantification was performed in triplicate and the level of expression of 18S rRNA was used as an internal control.

2.4. Phospho-RTK array and Western blot analysis

A Human Phospho-RTK Array Kit (R&D Systems, Minneapolis, MN) was used to measure the relative level of tyrosine phosphorylation of 42 distinct receptor tyrosine kinases (RTKs), according to the manufacturer's instructions as described previously [10].

The preparation of total cell lysates and immunoblotting was performed as described previously. Briefly, cells were cultured until subconfluent, and the medium was changed to 5% FBS containing dimethyl sulfoxide (DMSO) or the indicated concentration of the drug(s) for the durations indicated. Cells were rinsed in PBS, lysed in SDS sample buffer, and homogenized. The total cell lysate (30 μg) was subjected to SDS PAGE and transferred to Immobilon-P polyvinylidene difluoride membranes (Millipore, Bedford, MA). After blocking with 5% nonfat dry milk, the membranes were incubated with primary antibodies, washed with PBS, reacted with secondary antibodies, treated with ECL solution, and exposed to film. All antibodies were purchased from Cell Signaling Technology (Beverly, MA).

2.5. Senescence-associated β-galactosidase (SA-β-gal assay)

SA-β-gal activity was measured using an SA-β-gal staining kit purchased from BioVision Research Products (Mountain View, CA), according to the manufacturer's instructions. Senescent cells were identified as blue-stained cells by standard light microscopy.

3. Results

3.1. Establishment of in vitro CL-387,785-resistant cells

First, we analyzed the growth-inhibitory effects of CL-387,785 in HCC827 cells and in HCC827EPR.S10 cells (abbreviated as HCC827EPR cells), and we identified that both cell lines are sensitive to this drug (IC_{50}; <10 nM in HCC827 cells and 380 nM in HCC827EPR cells, Fig. 1A).

We then generated CL-387,785-resistant cells from HCC827EPR cells by growing the cells in increasing concentrations of CL-387,785 (from 100 nM to a final concentration of 1 μM) for up to 3 months *in vitro*, as described previously [9,10]. The resultant CL-387,785-resistant cells (designated HCC827CLR cells) were maintained in the presence of 1 μM CL-387,785.

We extracted RNA and genomic DNA from HCC827CLR cells and analyzed the mutations, amplification, and gene expression of the candidate genes. Mutation analyses revealed that HCC827CLR cells harbored the T790M mutation in a similar ratio of mutant versus wild-type alleles to that of HCC827EPR cells (Fig. 1B). In addition, the *EGFR* gene copy number in HCC827CLR cells, assessed using quantitative real-time PCR, was identical to that observed in HCC827 cells and in HCC827EPR cells (25.0, 24.8, and 26.0 times compared with normal genomic DNA). Because HCC827 cells and their descendants do not have wild-type *EGFR* allele, these results indicate that the copy number of T790M containing allele in HCC827CLR cells is identical to that in HCC827EPR cells. On the other hand, the *MET* gene copy number in HCC827CLR cells was also identical to that observed in HCC827 cells and in HCC827EPR cells (1.3, 1.5, and 1.9 times compared with normal genomic DNA). In addition, the MET-TKI PHA-665,752 did not restore CL-387,785 sensitivity in HCC827CLR cells (data not shown). We and others have shown recently that the epithelial to mesenchymal transition (EMT) is involved in the acquired resistance to EGFR-TKIs [13–15]. However, HCC827CLR cells showed strong E-cadherin and weak vimentin expression (Fig. 1C, right lane) in addition to a tightly

Please cite this article in press as: Suda K, et al. Conversion from the "oncogene addiction" to "drug addiction" by intensive inhibition of the EGFR and MET in lung cancer with activating *EGFR* mutation. Lung Cancer (2011), doi:10.1016/j.lungcan.2011.11.007

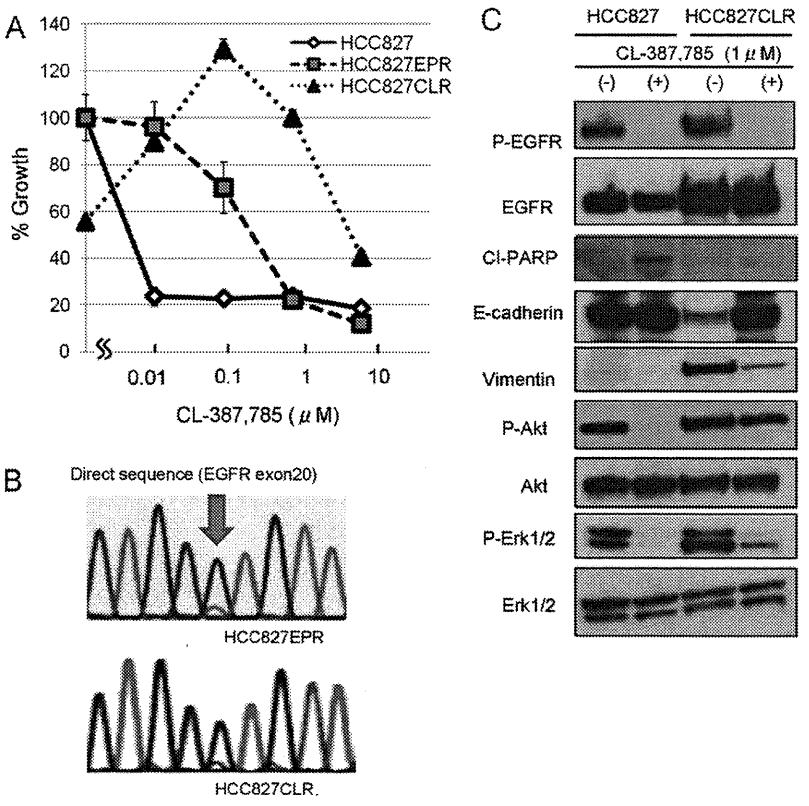

Fig. 1. Analysis of EGFR and candidate intracellular molecules in HCC827CLR cells. (A) Growth-inhibitory effect of CL-387,785. Percentage growth was calculated relative to DMSO-treated controls in HCC827 or HCC827EPR cells, and relative to 1 μM CL-387,785 (maintenance concentration) treated cells in HCC827CLR cells. (B) HCC827EPR and HCC827CLR cells harbored the T790M mutation in a similar mutant/wild-type allele ratio. Antisense strands of sequencing chromatograms for *EGFR* mRNA are shown. Blue arrow, C to T substitution at nucleotide 2369 (G to A on the antisense strand), which results in the T790M mutation. (C) Increased EGFR expression and maintained Akt phosphorylation in HCC827CLR cells. Western blotting was used to analyze HCC827 cells incubated for 24 h with DMSO or 1 μM CL-387,785, and HCC827CLR cells without CL-387,785 for two passages or those with continuous exposure to 1 μM CL-387,785. (For interpretation of the references to color in this figure legend, the reader is referred to the web version of this article.)

conjunct epithelial cell-like appearance (Fig. 2A), indicating that the acquired resistance in HCC827CLR cells was unrelated to the EMT.

3.2. *PTEN downregulation and restoration of CL-387,785 sensitivity by Akt inhibition in HCC827CLR cells*

In the analysis of downstream molecules of EGFR, we identified sustained phosphorylation of Akt in HCC827CLR cells in the presence of CL-387,785, although phosphorylation of ERK1/2 was inhibited effectively (Fig. 1C). First, we examined the relative expression of *PTEN* in these cells because *PTEN* downregulation and increased Akt phosphorylation have been reported to cause gefitinib resistance in PC9 cells [16]. As expected, HCC827CLR cells showed significant downregulation of *PTEN* expression, although that of HCC827EPR cells was similar to that of HCC827 cells (Fig. 3A). Therefore, we treated these cells with the Akt inhibitor, AKT 1/2 Kinase Inhibitor. The growth-inhibitory effect of AKT 1/2 Kinase Inhibitor alone was mild in HCC827, HCC827EPR, and HCC827CLR cells (Fig. 3B).

Next, we treated HCC827CLR cells with CL-387,785 combined with 1 μM AKT 1/2 Kinase Inhibitor. AKT 1/2 Kinase Inhibitor effectively suppressed Akt phosphorylation and increased cleaved PARP expression (Fig. 3C), and Akt inhibition restored CL-387,785 sensitivity (IC_{50}: 173 nM, Fig. 3D).

3.3. *"Drug addiction" and increased expression of the EGFR in HCC827CLR cells*

Further observation identified greater proliferation of HCC827CLR cells with 1 μM of CL-387,785 than with DMSO alone (the concentration of DMSO was the same in both experimental conditions; Fig. 1A). We also found marked morphological differences in HCC827CLR cells between those treated with (Fig. 2A) and without (Fig. 2B and C) CL-387,785. The morphological features observed in the cells without CL-387,785 included spindle-shaped cells, loss of intercellular connections, and increased formation of pseudopodia, suggesting the involvement of the EMT, and enlarged cells and flattened cell morphology within 1 week of drug withdrawal (Fig. 2C), suggesting the involvement of premature senescence.

We first used immunoblot analysis to analyze the protein expression of the EMT markers, EGFR, and its downstream molecules (Fig. 1C). Total EGFR expression was significantly higher in HCC827CLR cells, although CL-387,785 effectively suppressed the phosphorylation of EGFR in HCC827 and HCC827CLR cells. We also confirmed the significantly higher *EGFR* mRNA expression in HCC827CLR cells compared with HCC827 and HCC827EPR cells (Fig. 4A). However, *EGFR* gene copy number was identical in HCC827CLR, HCC827, and HCC827EPR cells as described above. Expression of cleaved PARP, one marker of apoptosis, was observed in HCC827 cells treated with CL-387,785 but not in HCC827CLR

Please cite this article in press as: Suda K, et al. Conversion from the "oncogene addiction" to "drug addiction" by intensive inhibition of the EGFR and MET in lung cancer with activating *EGFR* mutation. Lung Cancer (2011), doi:10.1016/j.lungcan.2011.11.007

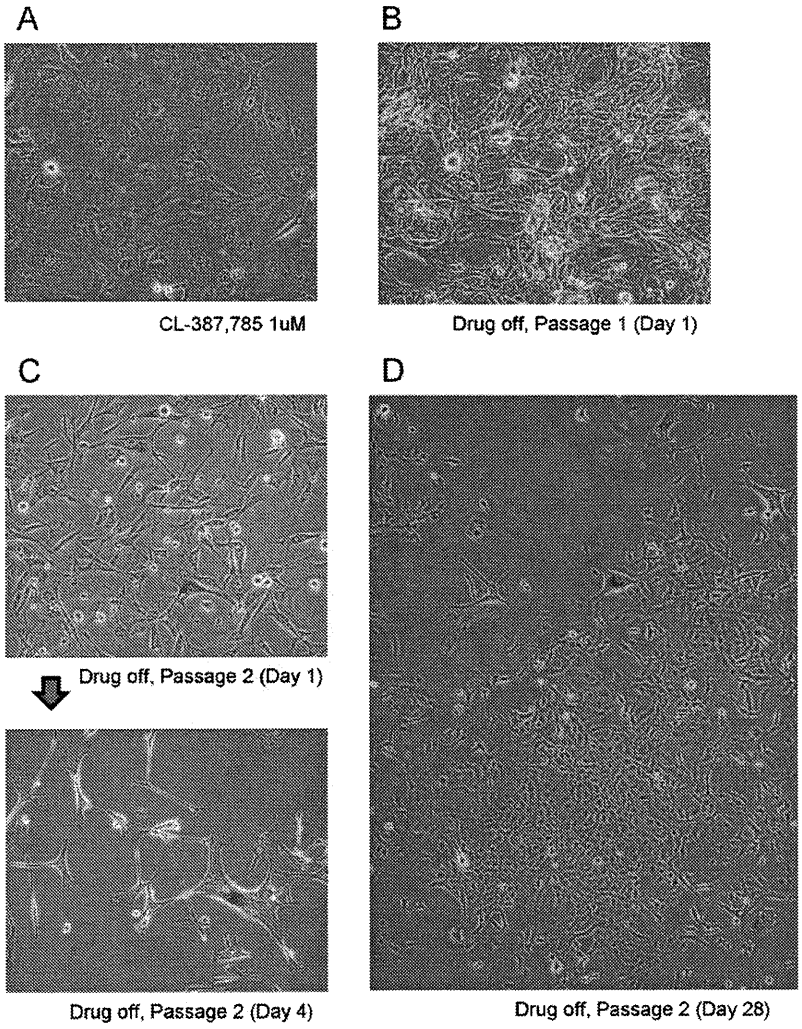

Fig. 2. Morphological differences between HCC827CLR cells treated with CL-387,785 (A), those not treated with CL-387,785 (B and C), and HCC827CLF cells (D) observed under standard light microscopy. Senescence-associated β-galactosidase is stained blue.

cells treated with or without CL-387,785 (Fig. 1C). HCC827CLR cells without CL-387,785 showed significantly increased expression of vimentin and downregulation of E-cadherin (Fig. 1C), which were consistent with their morphological changes.

3.4. Need for MEK inhibition for the maintenance of cell proliferation

Because Akt inhibition could not restore proliferation of HCC827CLR cells in the absence of CL-387,785 (Fig. 3A), we next analyzed the inhibitory effects of MEK–ERK pathway, the other main downstream signaling from the EGFR, using a MEK inhibitor PD0325901. Both HCC827 parental cells and HCC827EPR cells showed moderate sensitivity to this drug (Fig. 4C, left). Interestingly, PD0325901 restored the epithelial morphology in HCC827CLR cells without CL-387,785 treatment and restored cell proliferation in HCC827CLR cells without CL-387,785 (Fig. 4C, left). We performed the same experiments using another MEK inhibitor, ADZ6244, and obtained the same results (Fig. 4C, right). Western blot analysis showed that PD0325901 suppressed the phosphorylation of ERK1/2 more effectively than did AZD6244 (Fig. 4B); this result is consistent with the finding that PD0325901 has a greater "proliferation recovery effect" than does AZD6244.

3.5. Senescence reaction in HCC827CLR cells without EGFR inhibition

The growth-inhibitory effect of HCC827CLR cells caused by CL-387,785 withdrawal could not be explained by apoptosis (Fig. 1C). We next stained for SA-β gal in HCC827CLR cells with or without CL-387,785 because the following results suggested the involvement of oncogene-induced senescence: (i) the morphological changes described above were consistent with senescence, (ii) EGFR or ERK inhibition restored proliferation in HCC827CLR cells, and (iii) hyperactivation of the RAS–MEK–ERK pathway has been reported to cause oncogene induced senescence [17]. Few HCC827CLR cells treated with CL-387,785 (1.0%) were positive for SA-β gal (Fig. 2A), but many more HCC827CLR cells without CL-387,785 (9.4%) were positive for SA-β gal (Fig. 2B and C). These findings indicate that oncogene-induced senescence is one cause of this "drug addiction".

3.6. Establishment of HCC827CLF cells

As shown in Fig. 2C, many HCC827CLR cells died when they were maintained without CL-387,785. We cultured these cells (passage 2 after CL-387,785 withdrawal) without any passage until

Please cite this article in press as: Suda K, et al. Conversion from the "oncogene addiction" to "drug addiction" by intensive inhibition of the EGFR and MET in lung cancer with activating *EGFR* mutation. Lung Cancer (2011), doi:10.1016/j.lungcan.2011.11.007

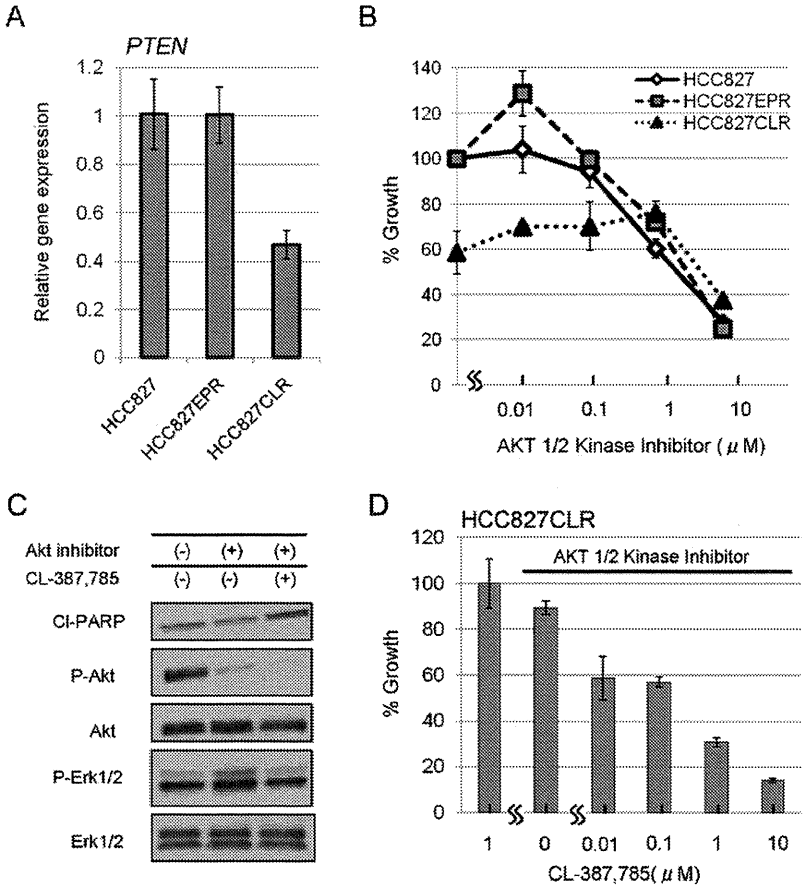

Fig. 3. Combined effect of AKT 1/2 Kinase Inhibitor and CL-387,785 in HCC827CLR cells. (A) Quantitative real-time RT-PCR identified HCC827CLR cells showed downregulation of *PTEN* expression. (B) Growth-inhibitory effect of Akt inhibitor monotherapy. Percentage growth was calculated relative to DMSO-treated controls in HCC827 or HCC827EPR cells, and relative to 1 μM CL-387,785-treated cells in HCC827CLR cells. (C) HCC827CLR cells were cultured for two passages without CL-387,785 and then incubated for 48 h with DMSO, 1 μM AKT 1/2 Kinase Inhibitor, or the combination of AKT 1/2 Kinase Inhibitor and 1 μM CL-387,785, and then analyzed by Western blotting. (D) HCC827CLR cells were sensitive to CL-387,785 in the presence of an Akt inhibitor. Percentage growth was calculated relative to 1 μM CL-387,785-treated cells.

the cells began to proliferate again. After 4 weeks, some colonies were observed, and these cells were designated HCC827CLF (CL-387,785-free) cells (Fig. 2D). In the mutational analysis, HCC827CLF cells harbored the T790M mutation in a similar ratio of mutant versus wild-type alleles compared with HCC827EPR cells and HCC827CLR cells (data not shown). HCC827CLF cells were negative for SA-β gal and could be maintained without CL-387,785. HCC827CLF cells preserved the mesenchymal phenotype (e.g., spindle-shaped morphology, expression of vimentin, and loss of E-cadherin, Fig. 5A), irrespective of the presence of CL-387,785. *EGFR* expression decreased to the same level as that observed in HCC827EPR cells in translational (Fig. 4A) and in transcriptional (Fig. 5A) levels. HCC827CLF cells were mildly resistant to CL-387,785; about 60% of cells survived in the presence of 1 μM CL-387,785 (Fig. 5B).

4. Discussion

The second-generation EGFR-TKIs that can irreversibly and covalently bind to cysteine 797 of the EGFR are expected to overcome the acquired resistance conferred by the T790M mutation [18]. The EGFR-TKIs that belong to this class (e.g., PF299804 and BIBW2992) are currently under clinical evaluation [18] and these drugs may be administered to some patients who acquire the T790M mutation. However, little is known about how cancer cells behave in this situation.

Ercan et al. generated PF299804-resistant cell lines from gefitinib-resistant PC9 cells (*EGFR* delE746_A750 with T790M) and found that amplification of *EGFR* T790M was the cause of the resistance [19]. In the present study, although our CL-387,785-resistant cells (HCC827CLR cells) did not harbor the T790M amplification (Fig. 1B), *PTEN* expression was downregulated and Akt phosphorylation was sustained in the presence of CL-387,785 (Fig. 1C). We also observed that Akt inhibition restored the sensitivity to CL-387,785 in HCC827CLR cells (Fig. 3D). Downregulation of *PTEN* has been reported to cause primary erlotinib resistance in *EGFR* mutant lung cancer cells [20], and to cause acquired resistance to gefitinib in PC9 cells [16]. We found that acquired resistance caused by *PTEN* downregulation occurred in an *EGFR*-mutant lung cancer cell line other than PC9 cells. We also found that *PTEN* downregulation was the mechanism responsible for "secondary" acquired resistance to EGFR-TKIs after the acquisition of the T790M mutation. Our results suggest that the combined inhibition of the PI3K–Akt pathway along with EGFR inhibition may be necessary in the treatment of *EGFR*-mutant lung cancers.

The other finding in this study was the "drug addiction" phenomenon in HCC827CLR cells. In other words, HCC827CLR cells were not only able to proliferate in the presence of CL-387,785, but also underwent senescence, as evidenced by the increased expression of SA-β gal upon withdrawal of CL-387,785. HCC827CLR cells showed increased *EGFR* expression. The senescence-inhibitory activity of CL-387,785 could be substituted by erlotinib. We also

Please cite this article in press as: Suda K, et al. Conversion from the "oncogene addiction" to "drug addiction" by intensive inhibition of the EGFR and MET in lung cancer with activating *EGFR* mutation. Lung Cancer (2011), doi:10.1016/j.lungcan.2011.11.007

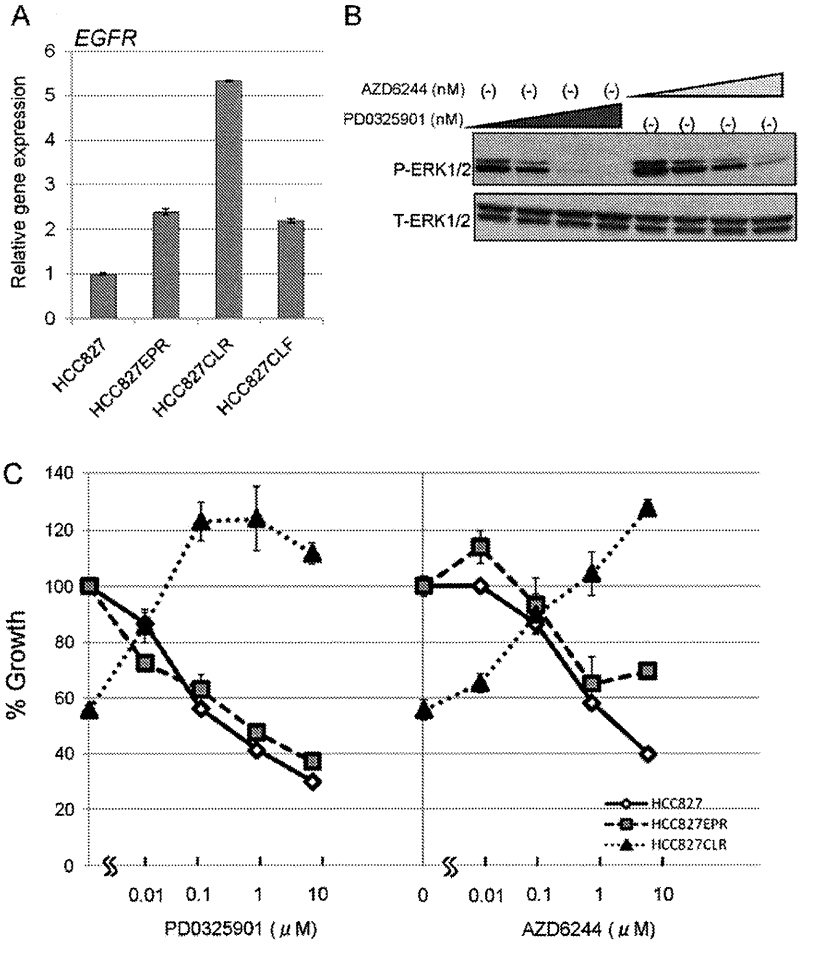

Fig. 4. Restoration of proliferation by MEK inhibitors in HCC827CLR cells not treated with CL-387,785. (A) *EGFR* gene expression increased in HCC827CLR cells. Relative gene expressions compared with HCC827 parental cells were analyzed by quantitative real-time RT-PCR. (B) HCC827CLR cells were cultured for two passages without CL-387,785 and then incubated for 48 h with the indicated concentrations (10 nM, 100 nM, 1000 nM, or 10000 nM) of PD0325901 or AZD6244, and examined by Western blotting. (C) Growth-inhibitory effect of MEK inhibitor monotherapy. Percentage growth was calculated relative to DMSO-treated controls in HCC827 or HCC827EPR cells, and relative to 1 μM CL-387,785-treated cells in HCC827CLR cells.

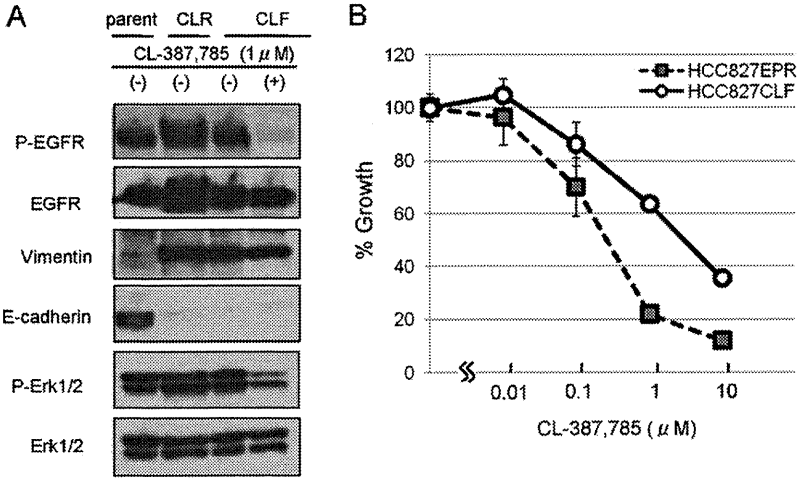

Fig. 5. Analysis of HCC827CLF cells. (A) HCC827CLF cells were incubated for 48 h with DMSO or 1 μM CL-387,785 and examined by Western blotting. (B) Growth-inhibitory effect of CL-387,785 in HCC827CLF cells. Percentage growth was calculated relative to DMSO-treated controls. The results for HCC827EPR cells (data from Fig. 1A) are shown for comparison.

Please cite this article in press as: Suda K, et al. Conversion from the "oncogene addiction" to "drug addiction" by intensive inhibition of the EGFR and MET in lung cancer with activating *EGFR* mutation. Lung Cancer (2011), doi:10.1016/j.lungcan.2011.11.007

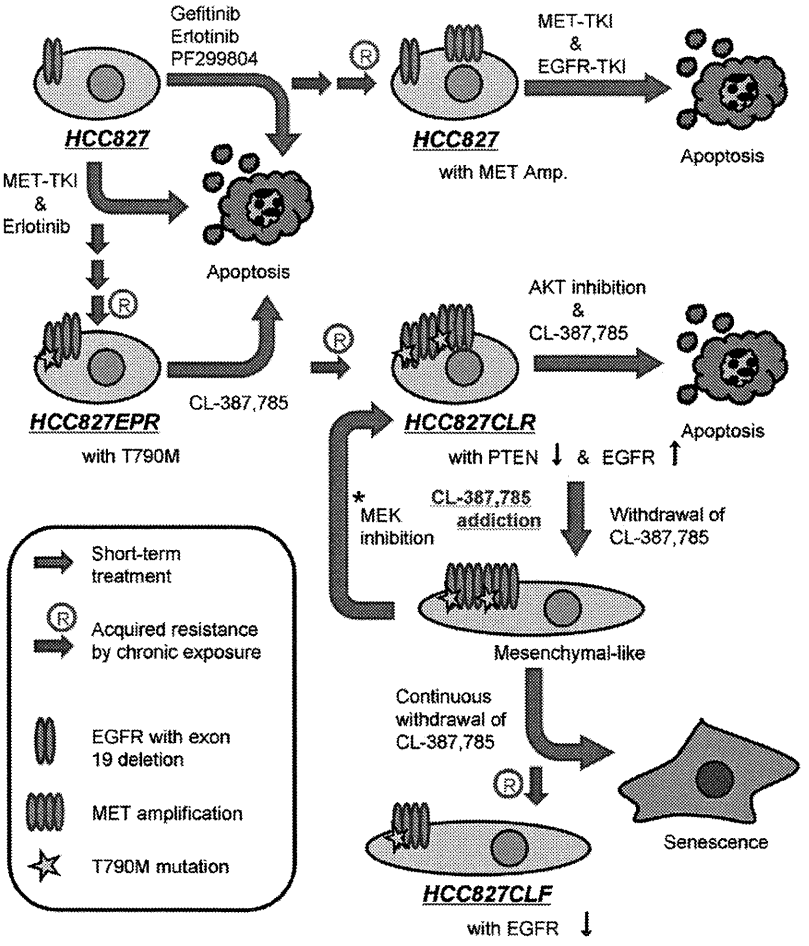

Fig. 6. Schema of the phenotypic changes in HCC827 lung cancer cells from "oncogene addiction" to "acquired resistance" and further to "drug addiction" during adaptation to intensive EGFR and MET kinase inhibition. HCC827CLR cells were addicted to CL-387,785 and withdrawal of CL-387,785 caused mesenchymal-like phenotype, and further, increased senescence. However, MEK inhibition restored cell proliferation in HCC827CLR cells without CL-387,785 (*).

found that MEK–ERK inhibition but not Akt inhibition could restore this activity. Because the KRAS–MEK–ERK pathway is reported to be related to senescence [17,21,22], we suggest that the mechanism responsible for this "drug addiction" is senescence by a hyperactivated EGFR–MEK–ERK pathway conferred by the sudden dysregulation of overexpressed *EGFR* upon withdrawal of CL-387,785. This is consistent with the result showing that EGFR expression in HCC827CLR cells returned to the same level as in the original HCC827EPR cells (Fig. 4A) and resumed to grow after a month of culture without the drug (HCC827CLF cells).

Fig. 6 illustrates how the HCC827 lung cancer cells behaved after intensive and sequential treatment with several TKIs. HCC827 cells had the potential to develop *MET* amplification, the T790M mutation, *EGFR* overexpression, *PTEN* downregulation, and the EMT so that they could adapt and survive in an environment with potent and selective TKI treatment. Although the overexpressed *EGFR* seemed to be a vulnerability in the absence of EGFR-TKIs, perhaps through oncogene-induced senescence, *EGFR* expression could decrease readily in HCC827CLR cells cultured in the drug-free condition.

This condition we call "drug addiction" contrasts with the so-called "flare effect" after withdrawal of EGFR-TKIs after the patient experiences progressive disease. Riely et al. analyzed ten patients with acquired resistance to EGFR-TKI and observed a median 18% increase in the SUVmax (standard uptake value) in positron emission tomography and 9% increase in tumor diameter, 3 weeks after stopping the EGFR-TKI [23]. However, we believe that, in some situations after intensive treatment with EGFR inhibitors, the opposite may occur as shown in our *in vitro* study.

In conclusion, we observed *PTEN* downregulation as an acquired resistance mechanism in HCC827CLR cells established through intensive and sequential TKI treatment. Our series of experiments highlights the flexibility of cancer cells that have adapted to environmental stresses induced by intensive and sequential treatment with potent and selective TKIs. Cancer cells sometimes become not only resistant to the TKI but also dependent on or addicted to the TKI. This highly flexible and plastic nature of the cancer cells should be considered when trying to improve the outcomes in patients with lung cancer.

Conflict of interest

Dr. Mitsudomi has received lecture fees from AstraZeneca and Chugai, and he is a member of advisory boards of Pfizer and Boehringer-Ingelheim. The other authors declare no conflict of interest.

Acknowledgments

This study is supported in part by a Grant-in-Aid for Scientific Research (B) from the Japan Society for the Promotion of Science

Please cite this article in press as: Suda K, et al. Conversion from the "oncogene addiction" to "drug addiction" by intensive inhibition of the EGFR and MET in lung cancer with activating *EGFR* mutation. Lung Cancer (2011), doi:10.1016/j.lungcan.2011.11.007

(20903076) and grant from the Kobayashi Institute for Innovative Cancer Chemotherapy.

References

[1] Mok TS, Wu YL, Thongprasert S, Yang CH, Chu DT, Saijo N, et al. Gefitinib or carboplatin–paclitaxel in pulmonary adenocarcinoma. N Engl J Med 2009;361:947–57.
[2] Mitsudomi T, Morita S, Yatabe Y, Negoro S, Okamoto I, Tsurutani J, et al. Gefitinib versus cisplatin plus docetaxel in patients with non-small-cell lung cancer harbouring mutations of the epidermal growth factor receptor (WJTOG3405): an open label, randomised phase 3 trial. Lancet Oncol 2010;11:121–8.
[3] Maemondo M, Inoue A, Kobayashi K, Sugawara S, Oizumi S, Isobe H, et al. Gefitinib or chemotherapy for non-small-cell lung cancer with mutated EGFR. N Engl J Med 2010;362:2380–8.
[4] Pao W, Miller VA, Politi KA, Riely GJ, Somwar R, Zakowski MF, et al. Acquired resistance of lung adenocarcinomas to gefitinib or erlotinib is associated with a second mutation in the EGFR kinase domain. PLoS Med 2005;2:e73.
[5] Kobayashi S, Boggon TJ, Dayaram T, Janne PA, Kocher O, Meyerson M, et al. EGFR mutation and resistance of non-small-cell lung cancer to gefitinib. N Engl J Med 2005;352:786–92.
[6] Engelman JA, Zejnullahu K, Mitsudomi T, Song Y, Hyland C, Park JO, et al. MET amplification leads to gefitinib resistance in lung cancer by activating ERBB3 signaling. Science 2007;316:1039–43.
[7] Sequist LV, Waltman BA, Dias-Santagata D, Digumarthy S, Turke AB, Fidias P, et al. Genotypic and histological evolution of lung cancers acquiring resistance to EGFR inhibitors. Sci Transl Med 2011;3, 75ra26.
[8] Yun CH, Mengwasser KE, Toms AV, Woo MS, Greulich H, Wong KK, et al. The T790M mutation in EGFR kinase causes drug resistance by increasing the affinity for ATP. Proc Natl Acad Sci USA 2008;105:2070–5.
[9] Turke AB, Zejnullahu K, Wu YL, Song Y, Dias-Santagata D, Lifshits E, et al. Preexistence and clonal selection of MET amplification in EGFR mutant NSCLC. Cancer Cell 2010;17:77–88.
[10] Suda K, Murakami I, Katayama T, Tomizawa K, Osada H, Sekido Y, et al. Reciprocal and complementary role of MET amplification and EGFR T790M mutation in acquired resistance to kinase inhibitors in lung cancer. Clin Cancer Res 2010;16:5489–98.
[11] Kosaka T, Yatabe Y, Endoh H, Kuwano H, Takahashi T, Mitsudomi T. Mutations of the epidermal growth factor receptor gene in lung cancer: biological and clinical implications. Cancer Res 2004;64:8919–23.
[12] Onozato R, Kosaka T, Kuwano H, Sekido Y, Yatabe Y, Mitsudomi T. Activation of MET by gene amplification or by splice mutations deleting the juxtamembrane domain in primary resected lung cancers. J Thorac Oncol 2009;4:5–11.
[13] Yao Z, Fenoglio S, Gao DC, Camiolo M, Stiles B, Lindsted T, et al. TGF-beta IL-6 axis mediates selective and adaptive mechanisms of resistance to molecular targeted therapy in lung cancer. Proc Natl Acad Sci USA 2010;107:15535–40.
[14] Suda K, Tomizawa K, Fujii M, Murakami H, Osada H, Maehara Y, et al. Epithelial to mesenchymal transition in an epidermal growth factor receptor-mutant lung cancer cell line with acquired resistance to erlotinib. J Thorac Oncol 2011;6:1152–61.
[15] Chung JH, Rho JK, Xu X, Lee JS, Yoon HI, Lee CT, et al. Clinical and molecular evidences of epithelial to mesenchymal transition in acquired resistance to EGFR-TKIs. Lung Cancer 2011;73:176–82.
[16] Yamamoto C, Basaki Y, Kawahara A, Nakashima K, Kage M, Izumi H, et al. Loss of PTEN expression by blocking nuclear translocation of EGR1 in gefitinib-resistant lung cancer cells harboring epidermal growth factor receptor-activating mutations. Cancer Res 2010;70:8715–25.
[17] Serrano M, Lin AW, McCurrach ME, Beach D, Lowe SW. Oncogenic ras provokes premature cell senescence associated with accumulation of p53 and p16INK4a. Cell 1997;88:593–602.
[18] Giaccone G, Wang Y. Strategies for overcoming resistance to EGFR family tyrosine kinase inhibitors. Cancer Treat Rev 2011;37:456–64.
[19] Ercan D, Zejnullahu K, Yonesaka K, Xiao Y, Capelletti M, Rogers A, et al. Amplification of EGFR T790M causes resistance to an irreversible EGFR inhibitor. Oncogene 2010;29:2346–56.
[20] Sos ML, Koker M, Weir BA, Heynck S, Rabinovsky R, Zander T, et al. PTEN loss contributes to erlotinib resistance in EGFR-mutant lung cancer by activation of Akt and EGFR. Cancer Res 2009;69:3256–61.
[21] Collado M, Gil J, Efeyan A, Guerra C, Schuhmacher AJ, Barradas M, et al. Tumour biology: senescence in premalignant tumours. Nature 2005;436:642.
[22] Boucher MJ, Jean D, Vezina A, Rivard N. Dual role of MEK/ERK signaling in senescence and transformation of intestinal epithelial cells. Am J Physiol 2004;286:G736–46.
[23] Riely GJ, Kris MG, Zhao B, Akhurst T, Milton DT, Moore E, et al. Prospective assessment of discontinuation and reinitiation of erlotinib or gefitinib in patients with acquired resistance to erlotinib or gefitinib followed by the addition of everolimus. Clin Cancer Res 2007;13:5150–5.

Please cite this article in press as: Suda K, et al. Conversion from the "oncogene addiction" to "drug addiction" by intensive inhibition of the EGFR and MET in lung cancer with activating *EGFR* mutation. Lung Cancer (2011), doi:10.1016/j.lungcan.2011.11.007

Published OnlineFirst August 19, 2011; DOI:10.1158/0008-5472.CAN-11-1020

Molecular and Cellular Pathobiology

Cancer Research

miR-375 Is Activated by ASH1 and Inhibits YAP1 in a Lineage-Dependent Manner in Lung Cancer

Eri Nishikawa[1], Hirotaka Osada[2,4], Yasumasa Okazaki[3], Chinatsu Arima[1], Shuta Tomida[1], Yoshio Tatematsu[4], Ayumu Taguchi[1], Yukako Shimada[1], Kiyoshi Yanagisawa[6], Yasushi Yatabe[5], Shinya Toyokuni[3], Yoshitaka Sekido[2,4], and Takashi Takahashi[1]

Abstract

Lung cancers with neuroendocrine (NE) features are often very aggressive but the underlying molecular mechanisms remain elusive. The transcription factor ASH1/ASCL1 is a master regulator of pulmonary NE cell development that is involved in the pathogenesis of lung cancers with NE features (NE-lung cancers). Here we report the definition of the microRNA *miR-375* as a key downstream effector of ASH1 function in NE-lung cancer cells. *miR-375* was markedly induced by ASH1 in lung cancer cells where it was sufficient to induce NE differentiation. *miR-375* upregulation was a prerequisite for ASH1-mediated induction of NE features. The transcriptional coactivator YAP1 was determined to be a direct target of *miR-375*. YAP1 showed a negative correlation with *miR-375* in a panel of lung cancer cell lines and growth inhibitory activities in NE-lung cancer cells. Our results elucidate an ASH1 effector axis in NE-lung cancers that is functionally pivotal in controlling NE features and the alleviation from YAP1-mediated growth inhibition. *Cancer Res; 71(19); 6165–73. ©2011 AACR.*

Introduction

Lung cancer has long been the leading cause of cancer-related death in economically developed countries, and a better understanding of the molecular pathogenesis of this fatal disease is greatly anticipated for preventive and/or therapeutic breakthroughs (1). Accumulated evidence strongly suggests that alterations of microRNA (miRNA) expressions are involved in the development of human cancers (2–5). Our previous studies identified *let-7* as a miRNA family with growth inhibitory activities, which were also found to be frequently downregulated in lung cancers in association with poor prognosis (6). In marked contrast to the tumor suppressor-like *let-7* miRNA family, the *miR-17-92* miRNA cluster plays roles as oncogene-type miRNAs in the development of lung cancers (7, 8).

Lung cancer is classified into 2 major classes, small cell lung cancer (SCLC) and non-SCLC (NSCLC), of which SCLC characteristically exhibits neuroendocrine (NE) features and an aggressive clinical course. In addition, a small proportion of NSCLCs such as large cell NE carcinoma also share such characteristics. Therefore, it is conceivable that elucidation of the underlying mechanisms involved in the acquisition of those characteristics in lung cancers with NE features may provide important clues for a better understanding of carcinogenic processes. Along this line, we previously reported that A549 lung adenocarcinoma cells exhibited NE properties when introduced with achaete-scute homologue 1 (ASH1/ASCL1), a proneural basic helix-loop-helix (bHLH) transcription factor (9), whereas ASH1 knockdown elicited prominent apoptosis in SCLC lung cancer cell lines (10). We also found that ASH1 mediates lineage-survival signal in SCLC at least in part through its transcriptional repressor activity toward putative tumor suppressor including *DKK1* and *E-cadherin* (9). However, to date, virtually nothing is known about the possible involvement of miRNAs downstream of this dual function transcription factor, which is crucially involved in the biology of SCLC.

In this study, we investigated whether miRNAs are also governed by ASH1 and have roles downstream of ASH1 downstream in the development of lung cancers with NE features. Consequently, *miR-375* was identified as a miRNA directly and highly transactivated by ASH1. The involvement of *miR-375* in acquisition of NE phenotypes and growth regulation in lung cancers with NE features is also discussed.

Authors' Affiliations: [1]Division of Molecular Carcinogenesis, Center for Neurological Diseases and Cancer, [2]Department of Cancer Genetics, Program in Function Construction Medicine, and [3]Department of Pathology and Biological Responses, Nagoya University Graduate School of Medicine; [4]Division of Molecular Oncology, Aichi Cancer Center Research Institute; [5]Department of Pathology and Molecular Diagnostics, Aichi Cancer Center Hospital; and [6]Institute for Advanced Research, Nagoya University, Nagoya, Japan

Note: Supplementary data for this article are available at Cancer Research Online (http://cancerres.aacrjournals.org/).

E. Nishikawa and H. Osada contributed equally to this work.

Corresponding Author: Takashi Takahashi, Division of Molecular Carcinogenesis, Center for Neurological Diseases and Cancer, Nagoya University Graduate School of Medicine, Nagoya, Japan. E-mail: tak@med.nagoya-u.ac.jp or Hirotaka Osada, Aichi Cancer Center Research Institute, Nagoya, Japan. E-mail: hosada@aichi-cc.jp

doi: 10.1158/0008-5472.CAN-11-1020

Published OnlineFirst August 19, 2011; DOI:10.1158/0008-5472.CAN-11-1020

Materials and Methods

Cells and expression constructs

An A549 lung adenocarcinoma cell line without NE differentiation and a typical SCLC cell line, ACC-LC-172, as well as A549 cells stably transduced with ASH1-expressing (A549-ASH1) or empty (A549-VC) lentiviruses (9) were maintained in RPMI-1640 with 5% FBS. ASH1-expressing lentiviral and plasmid vectors were constructed with CSII-CMV-MCS-IRES2-Blasticidin and pcDNA3 (Invitrogen), respectively, as previously described (9). Yes-associated protein 1 (YAP1) cDNA was purchased from OriGene and inserted into CSII-EF-MCS-IRES2-Venus. The lentivirus vectors were kindly provided by Dr. H. Miyoshi (RIKEN BioResource Center). Venus (improved YFP) was provided by Dr. A. Miyawaki (RIKEN Brain Science Institute).

Reporter assay

A 1,028-bp-long putative promoter fragment spanning from 992 bp upstream of the *pre-miR-375* sequence to 3 bp upstream of the mature *miR-375* sequence was amplified from human genomic DNA and cloned into a pGL4.10 basic reporter (pGL4-375P in Fig. 1B). pGL4-Δ1, -Δ2, and -Δ3 truncated reporter plasmids were constructed by reamplification of the pGL4-375P plasmid, with each containing 103, 324, and 681 bp regions 5′ to the *pre-miR-375* sequence (Fig. 1B; Supplementary Fig. S1B). E-box deletion mutant reporters were also constructed by PCR-mediated *in vitro* mutagenesis of pGL4-Δ3. Each of these *miR-375* promoter reporters was transfected into A549 cells using Lipofectamine 2000 (Invitrogen) together with an ASH1 expression vector, pcDNA3-ASH1, or control empty vector, pcDNA3, with the renilla luciferase reporter pRL-TK used as an internal control.

microRNA microarray and gene expression microarray analysis

Microarray analysis was conducted to examine miRNA expression profiles using a Human miRNA Microarray, precommercial version 6.0 (Agilent) with 470 miRNA probes, according to the manufacturer's instructions. A549 cells were infected with an ASH1-expressing or empty lentivirus and harvested 4 days later. miRNA microarray data were $\log_2$ transformed and normalized to the 75th percentile. Microarray analysis by a Whole Human Genome 4 × 44K Microarray G4112F (Agilent) was also conducted to examine changes in expression of potential target genes of *miR-375* by transfection of Pre-miR-375 or Pre-miR-NC#2 (Ambion) in A549 cells, which were then harvested at 12, 24, 48, and 96 hours after transfection. RNA samples were prepared by using an RNeasy kit (Qiagen) as previously described. All the microarray data used for this study are available at Gene Expression Omnibus accession numbers GSE31565 and GSE31566).

Quantitative reverse transcriptase PCR

Quantitative reverse transcriptase PCR (RT-PCR) analysis was carried out by using primers for chromogranin A (CHGA), chromogranin B (CHGB), secretogranin II (SCG2), secretogranin III (SCG3), ASH1, YAP1, and β-actin (Supplementary Table S1), along with Power SYBR Green PCR Master Mix (Applied Biosystems), and an ABI Prism7500 (Applied Biosystems), as previously described. Expression levels were calculated by using the standard curve method and normalized with the expression of β-actin. The expression of *miR-375* was determined by quantitative RT-PCR analysis by using a TaqMan MicroRNA Assay and TaqMan MicroRNA RT Kit (Applied Biosystems). The expression level of *miR-375* was normalized with that of the noncoding RNA *RNU48*.

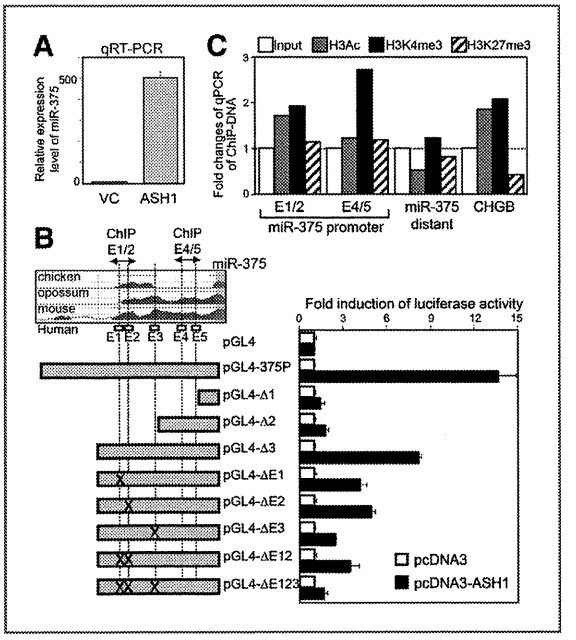

Figure 1. Characterization of the putative *miR-375* promoter. A, induction of *miR-375* by ASH1. The expression of miRNAs in ASH1-infected A549 was determined by microRNA quantitative RT-PCR analyses. B, reporter assay. Putative *miR-375* promoter reporters were transfected into A549 cells together with an ASH1 expression vector, pcDNA3-ASH1, or a control empty vector, pcDNA3. The reporter plasmids pGL4-Δ1, -Δ2, and -Δ3 contain promoter fragments that are 103, 324, and 681 bp upstream from the start site of *pre-miR-375*, as indicated in Supplementary Figure S1B. Deletions of conserved E-boxes (E1–E5) are indicated by "X" marks. C, quantitative ChIP assay. ChIP assays with antibodies against various histone H3 modifications were carried out by A549-ASH1 and ASH1-VC cells. PCR products of the ChIP E1/2 and ChIP E4/5 regions, indicated by arrows in (B), were measured. The ratios of A549-ASH1 cells against A549-VC cells are shown as fold changes. PCR findings for both ChIP E1/2 and ChIP E4/5 showed increases in activation of histone modifications (H3Ac and H3K4me3) in the *miR-375* promoter, whereas distant primers did not show any activating histone modifications.

Quantitative ChIP assay

ChIP assays were carried out as described previously, using ChIP E1/2 and ChIP E4/5 primers, which were designed for amplification of genomic fragments containing E1 and E2 E-boxes and E4 and E5 E-boxes, respectively (Fig. 1B). ChIP analysis using "distant" primers for amplification of a genomic

Published OnlineFirst August 19, 2011; DOI:10.1158/0008-5472.CAN-11-1020

region approximately 5.3 kb downstream of *pre-miR-375* (Supplementary Fig. S1) as well as CHGB primers were used as negative and positive controls, respectively. The primer sequences are shown in Supplementary Table S1. The amounts of chromatin-immunoprecipitated genomic DNA were measured by the ΔΔCt method to compare various ChIP primers and β-actin primers and the results of quantification were obtained as fold changes of A549-ASH1 against A549-VC. Antibodies against acetylated histone H3 (H3Ac), trimethylated H3 lysine 4 (H3K4me3), and trimethylated H3 lysine 27 (H3K27me3) were purchased from Upstate.

In situ hybridization

We employed a Fluorescein isothiocyanate–labeled locked nucleic acid (LNA) probe for *mmu–miR-375* and a scrambled sequence (Exiqon). Probes were diluted to 40 nmol/L in hybridization buffer (Ambion). *In situ* hybridization was conducted according to the manufacturer's protocol, as previously described (11). In brief, after deparaffinization, neutral formalin-fixed specimens on slides were incubated in proteinase K solution (20 μg/mL) at 37°C. After fixing the specimens with 4% paraformaldehyde, endogenous peroxidase activities were quenched in methanol containing H_2O_2 [0.3% (v/v)], then the probes were hybridized overnight at 37°C. After washing with SSC with 50% formamide, a CSA II biotin-free catalyzed signal amplification system (Dako) was used to visualize miRNA expression as brown precipitates. Nuclear staining was done with hematoxylin.

Immunohistochemical analysis

Slides were subjected to an antigen retrieval procedure by using Immunosaver (Nisshin EM) and then endogenous peroxidase activities were quenched. Next, the slides were incubated with rabbit polyclonal antisynaptophysin antibody (Dako) followed by goat anti-rabbit immunoglobulins/horseradish peroxidase (Dako), and then visualized with liquid 3,3′-diaminobenzidine (Dako). Nuclear counterstaining was done with hematoxylin.

Transfection of Pre-miR-375 and LNA

Both Pre-miR-375 and Pre-miR-NC#2 were purchased from Ambion. Antisense and scramble oligonucleotides against mature *miR-375* were synthesized by using LNAs (Greiner). Each of oligonucleotides was introduced into A549 cells at 10 to 15 nmol/L, using 2.5 μL/mL of Lipofectamine RNAiMax (Invitrogen) according to the instructions of supplier.

Results

This study was initiated to investigate the potential involvement of miRNAs downstream of ASH1 in acquisition of characteristics of lung cancers with NE features. To this end, we first carried out genome-wide expression profiling of miRNAs to search for those significantly affected by ASH1 transduction in a lung cancer cell line without NE features. As a result, we identified 12 upregulated (>5-fold) and 8 downregulated (>5-fold) miRNAs in ASH1-transduced A549 cells (Table 1), of which *miR-375* was found to be the most highly

Table 1. Up- and downregulated miRNAs in ASH1-transduced A549 cells

miRNA	A549-ASH1[a]	A549-VC[a]	Fold change
Upregulated miRNAs (>5-fold)			
hsa-miR-375	62.806	0.038	1,659.802
hsa-miR-193a	8.071	0.726	11.120
hsa-miR-489	0.332	0.030	11.105
hsa-miR-10a	13.254	1.333	9.940
hsa-miR-196b	0.231	0.030	7.731
hsa-miR-181a	4.906	0.683	7.188
hsa-miR-181a*	0.185	0.026	7.108
hsa-miR-95	0.178	0.026	6.830
hsa-miR-326	0.353	0.052	6.785
hsa-miR-9*	2.559	0.397	6.441
hsa-miR-628	0.149	0.026	5.720
hsa-miR-181b	8.344	1.512	5.517
Downregulated miRNAs (>5-fold)			
hsa-miR-200b	0.018	1.008	0.018
hsa-miR-30a-3p	0.018	0.608	0.029
hsa-miR-137	0.018	0.467	0.038
hsa-miR-200a	0.018	0.455	0.039
hsa-miR-30a-5p	1.092	13.985	0.078
hsa-miR-149	0.116	1.363	0.085
hsa-miR-618	0.041	0.255	0.161
hsa-miR-422b	0.463	2.485	0.186

[a]Normalized signal intensity.

Published OnlineFirst August 19, 2011; DOI:10.1158/0008-5472.CAN-11-1020

upregulated, which was also verified by quantitative RT-PCR, using an *miR-375*–specific TaqMan probe (Fig. 1A). An ASH1 lentivirus was also transduced into 4 other NSCLC cell lines, 3 of which showed marked *miR-375* induction (Supplementary Fig. S2A). A survey of the genomic region harboring *miR-375* indicated that this miRNA resides in an intergenic region between the *CCDC108* and *CRVBA2* genes at chromosome 2q35 (Supplementary Fig. S1A), whereas a region approximately 1 kb in length was found to be evolutionally highly conserved (shown in red). Of the 5 conserved E-boxes, 4 were CACCTG whereas the other (E2) was CATCTG. To verify the promoter activity and responsiveness to ASH1, luciferase reporter constructs of the putative *miR-375* promoter and its various mutants were cotransfected with an ASH1 expression vector, pcDNA3-ASH1, or an empty vector into A549 cells. The pGL4-375P showed marked transactivation by ASH1 (Fig. 1B). pGL4-Δ3 containing 3 E-boxes (E1 to E3) showed robust responsiveness to ASH1, whereas pGL4-Δ2 with a further deletion failed to respond. Reporters, each of which contained a single E-box deletion mutation (pGL4-ΔE1, -ΔE2, and -ΔE3), showed moderate reductions in ASH1 responsiveness, whereas pGL4-ΔE123, carrying a deletion of all 3 E-boxes (E1 to E3), lost responsiveness to a level similar to that of pGL4-Δ2, indicating their crucial involvement in ASH1 responsiveness. To further confirm the promoter activity of this region, ChIP assays with antibodies against various histone H3 modifications were carried out by A549 cells infected with either ASH1-carrying or empty viruses (Fig. 1C). Consequently, specific induction of activating histone modifications (H3Ac and H3K4me3) in the genomic regions encompassing these 3 E-boxes were clearly shown in ASH1-expressing A549 cells. In addition, a ChIP assay with an anti–myc-tag antibody against the myc-tagged ASH1 protein indicated a direct interaction of ASH1 with the E1/2 region (Supplementary Fig. S3).

The association between ASH1 and *miR-375* expression was then analyzed in fetal mouse lung (Fig. 2A). Although neuroepithelial bodies (NEB), known to consist of ASH1-expressing pulmonary NE cells and epithelial progenitor cells (12), showed positive immunohistochemical staining for the NE marker synaptophysin, *in situ* hybridization showed coexpression of *miR-375*, showing that ASH1–*miR-375* signal is associated with NE differentiation. We also noted that *miR-375* was also detectable in pancreatic islet cells despite a lack of ASH1 expression, suggesting other mechanisms for its induction in the pancreas (Supplementary Fig. S4A). We observed histologic type-dependent expression of *miR-375* in the present lung cancer cell lines (Fig. 2B). A high level of expression was specifically detected in SCLC cell lines, which generally express ASH1 and have NE features (Fig. 2B). A moderate expression of *miR-375* was observed in large cell carcinoma cell lines, whereas *miR-375* was detected in a few exceptional adenocarcinoma cell lines, but in none of the squamous carcinoma cell lines. In addition, a positive correlation was seen between *miR-375* and ASH1 expression in the lung cancer cell lines (data not shown). Our *in situ* hybridization analysis revealed a positive signal for *miR-375* in the ACC-LC-172 SCLC cell line, whereas A549 did not show any signals (Supplementary Fig. S4B and C).

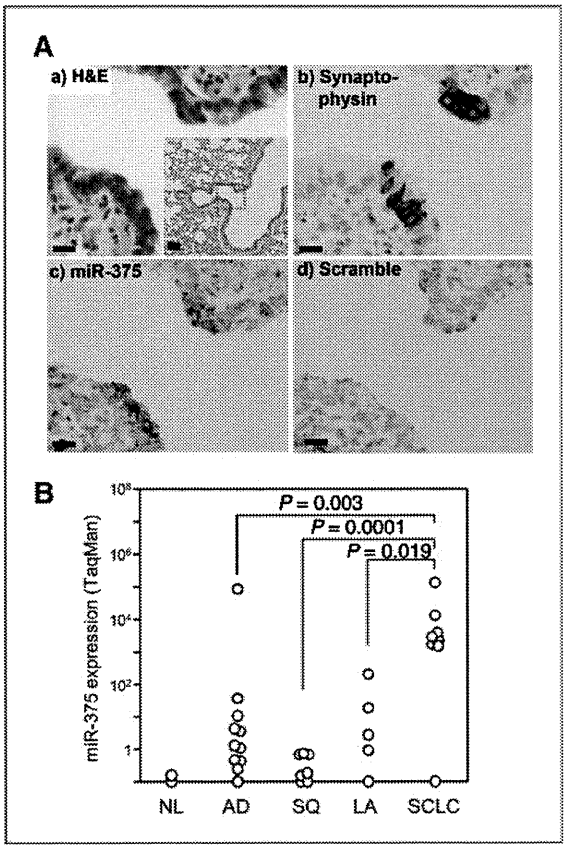

Figure 2. *miR-375* expression in normal lung and lung cancers. A, *in vivo* expression of *miR-375* in NEBs from fetal mouse lung tissue. a, hematoxylin and eosin (H&E) staining of normal fetal lung tissue containing 2 NEBs. The area with 2 NEBs enclosed by a red line is shown magnified in (a–d). b, IHC staining with antibody against the NE marker, synaptophysin. c and d, *in situ* hybridization with an *miR-375* antisense oligo (c) and scramble control oligo (d). Combinational analyses with IHC and *in situ* hybridization results showed restricted expressions of synaptophysin, and *miR-375* in NEBs. a (inset), magnification, 4×; black bar, 50 μm. a–d, magnification, 40×; black bar, 10 μm. B, expression levels of *miR-375* in lung cancer cell lines. NL, normal lung; AD, adenocarcinoma; SQ, squamous cell carcinoma; LA, large cell carcinoma. The SCLC cell lines showed significantly elevated expression of *miR-375*, whereas only moderate expression was observed in most of the LA cells. Only a few AD cell lines showed the expression of *miR-375*. Overexpression of *miR-375* in SCLC was statistically significant as compared with that expression in lung cancers of other histologic types.

We next investigated the functional significance of ASH1-inducible *miR-375* in terms of biological phenotypes of ASH1-positive lung cancer cells. To this end, we conducted genome-wide expression profiling analysis of *miR-375*–transfected A549 cells (Fig. 3A). Two hundred fifty-three genes exhibited greater than 2-fold changes in their expression levels between 12 and 96 hours after transfection. Interestingly, we noted that multiple NE-related genes were gradually induced at 48 and 96 hours after *miR-375* introduction, which was also confirmed by quantitative RT-PCR analysis results (Fig. 3B). As this finding strongly suggests that *miR-375* alone is capable of inducing NE

Published OnlineFirst August 19, 2011; DOI:10.1158/0008-5472.CAN-11-1020

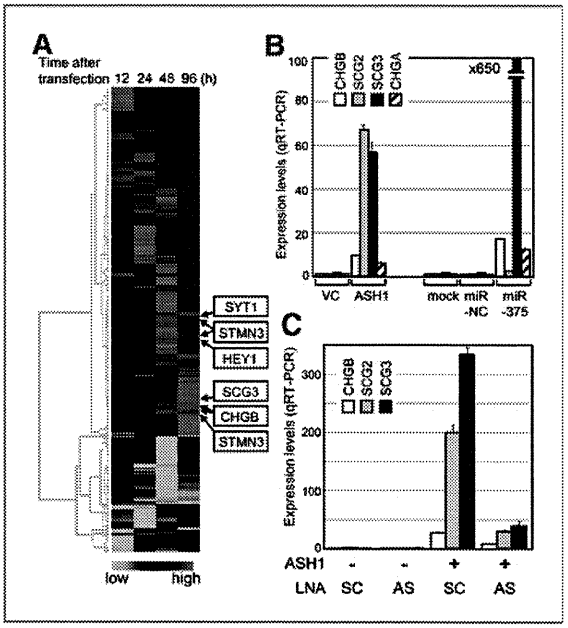

Figure 3. Gene expression profiling and NE induction after Pre-miR-375 transfection. A, the expression ratio of each gene of Pre-miR-375–transfected cells to those of Pre-miR-NC#2–transfected cells was analyzed by clustering. Time course (12–96 hours) of gene expression profiles after Pre-miR-375 transfection. Two hundred fifty-three genes showed greater than 2-fold changes in expression level. Genes related to NE features were indicated. SYT1, synaptotagmin I; STMN3, stathmin-like 3; HEY1, hairy/enhancer-of-split related with YRPW motif 1; SCG3, secretogranin III. B, induction of NE markers by *miR-375*. The expressions of NE markers were measured by quantitative RT-PCR. A549 cells transfected with Pre-miR-375 showed strong induction of NE markers as well as A549-ASH1 cells. C, inhibition of NE markers by *miR-375* antisense LNA. First, infection was performed with an ASH1-expressing or empty lentivirus, then *miR-375* antisense or scramble LNA was transfected into A549 cells. Strong inductions of NE markers by ASH1 were significantly inhibited by *miR-375* antisense LNA. AS, antisense; SC, scramble.

markers in the absence of ASH1, we then investigated whether *miR-375* is required for NE marker induction by ASH1. A549 cells were first infected with an ASH1-expressing lentivirus and subsequently transfected with *miR-375* antisense or scramble LNAs, which resulted in marked inhibition of ASH1-mediated induction of various NE markers in the presence of *miR-375* antisense, but not negative control, *miR-375* scramble (Fig. 3C). These findings clearly showed that ASH1-inducible *miR-375* is required for NE marker induction by ASH1 in lung cancer cells. To verify the specificity of NE marker induction by *miR-375*, we also transfected unrelated miRNAs into A549 cells. As shown in Supplementary Fig. S2B, various unrelated miRNAs scarcely induced CHGB expression, suggesting the specificity of *miR-375*–mediated NE marker induction. In addition, *miR-375* was transfected into 2 other NSCLC cell lines and 2 immortalized normal lung epithelial cell lines, HPL1D and BEAS2B, which confirmed CHGB induction at varying degrees in all 4 cell lines (Supplementary Fig. S2C).

To study the direct effects of *miR-375*, we analyzed changes in the expression profiles of target genes for *miR-375* predicted with TargetScan4.1 (http://www.targetscan.org/) and observed leftward shifts of the expression profile histograms, especially at 24 and 48 hours after *miR-375* transfection (Fig. 4A), which indicated moderate but significant downregulation of the predicted target genes of *miR-375*. In contrast, histograms of genes residing in chromosome 1 did not show any shifts, confirming specificity. Among the potential target genes affected by *miR-375*, transcriptional coactivator YAP1 was the most significantly repressed after *miR-375* transfection (Fig. 4B), which was also confirmed by Western blotting analysis (Fig. 4C). Two potential *miR-375* binding sites were also noted within the 3′-UTR of YAP1 mRNA, thus we carried out a luciferase assay by using YAP1 3′-UTR reporters (miR-375 × 1 and miR-375 × 2) containing either 1 or 2 potential *miR-375* binding sites (Fig. 4D). A549 cells transfected with these reporter constructs along with either Pre-miR-375 or negative control Pre-miR-NC#2 showed significant suppression of luciferase activity in a target site-dependent manner. The YAP1 3′-UTR reporter with deletion of the potential *miR-375* binding site abrogated *miR-375*–mediated suppression of luciferase activity (Supplementary Fig. S5A). The specificity of the *miR-375* target sites was also supported by our findings of lack of suppression of the wild-type YAP1 3′-UTR reporter activity by various unrelated miRNAs (Supplementary Fig. S5B). The relationship of *miR-375* with YAP1 was also substantiated by the significant negative correlation ($R = 0.793$, $P < 0.0001$) between *miR-375* and YAP1 in a panel of 29 lung cancer cell lines and 2 immortalized normal airway epithelial cell lines (Fig. 4E, left). In addition, we observed a histologic type-dependent expression pattern with low YAP1 expression in SCLC and abundant expression in NSCLC cell lines, indicating an expression pattern opposite to that of *miR-375*, which has abundant expression in SCLC (Fig. 4E, right). These relationships among ASH1, *miR-375*, and YAP1 were also observed in primary lung cancer specimens (Fig. 4F), suggesting the existence of robust regulatory relationships in the ASH1–*miR-375*–YAP1 pathway in lung cancers with NE features.

The negative correlation between *miR-375* and YAP1 found in a histologic type-related manner prompted us to investigate YAP1 functions in lung cancer cells of both histologic types. A549 adenocarcinoma and ACC-LC-172 SCLC cell lines were infected with YAP1-expressing or an empty lentivirus expressing the fluorescent protein Venus from an internal ribosomal entry site. Fluorescent microscopic examination revealed marked reduction of the fluorescence-positive population, which was indicative of successful infection by the YAP1-expressing virus, in contrast to robust growth in fluorescence-negative uninfected ACC-LC-172 cells (Fig. 5A), which we also confirmed by fluorescence-activated cell sorting analysis (Fig. 5B). In contrast to ACC-LC-172, A549 cells seemed to be tolerant to the introduction of YAP1, because the fluorescence-positive YAP1-infected population gradually increased (Fig. 5B). Time courses of fluorescent signals in lentivirus-infected A549 and ACC-LC172 cells are shown in Supplementary Figure S6A. YAP1-virus infection significantly inhibited the increase of fluorescent signals in ACC-LC-172 cells, but not in A549, suggesting a lineage-dependent growth-suppressive effect of YAP1. These findings were also confirmed by Western

Published OnlineFirst August 19, 2011; DOI:10.1158/0008-5472.CAN-11-1020

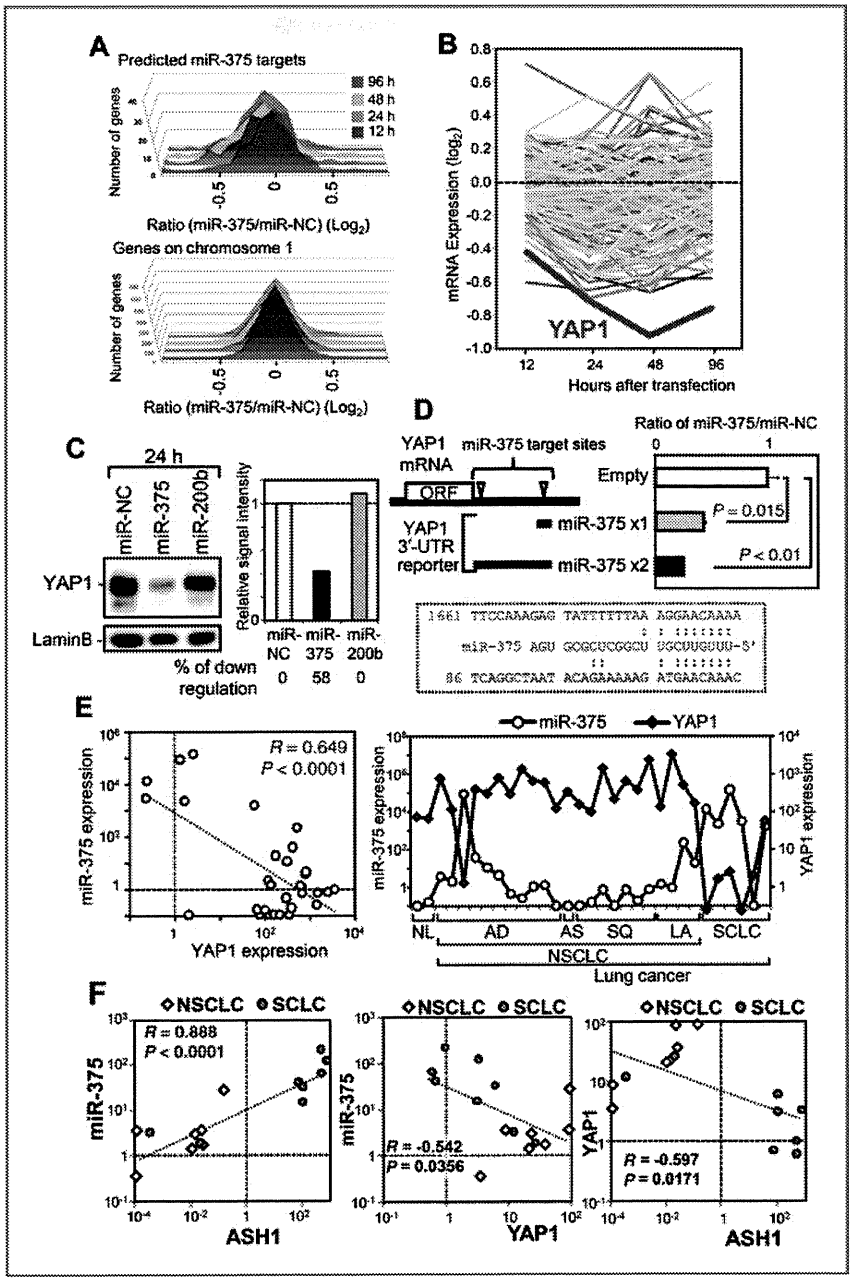

Figure 4. YAP1 inhibition by *miR-375*. A, histogram of gene expressions at 4 time points after Pre-miR-375 transfection. Gene expressions at 12 to 96 hours after transfection are shown as $\log_2$ ratio values between A549 cells transfected with Pre-miR-375 and Pre-miR-NC#2. Top, *miR-375* predicted target genes; bottom, genes residing in chromosome 1, which was used as a control. B, time course of expression of each *miR-375* predicted target gene after Pre-miR-375 transfection. C, Western blotting analysis of YAP1 protein. A549 cells transfected with Pre-miR-RNAs (15 nmol/L) were analyzed by Western blotting with the antibody against endogenous YAP1 protein. The intensity of YAP1 bands was determined with a densitometer and normalized with lamin B bands. Pre-miR-375 transfection downregulated the level of YAP1 protein by 58%. This downregulation is shown with a bar graph, in which the extent of downregulation is also numerically indicated. D, YAP1 3′-UTR reporter assay. YAP1 mRNA contains 2 *miR-375* target sites at the 3′-UTR. Two reporter constructs, miR-375 × 1 and miR-375 × 2, carry 1 and 2 *miR-375* sites, respectively. A549 cells were transfected with reporter constructs and Pre-miR-RNAs (10 nmol/L). The ratio of luciferase activity of Pre-miR-375 transfectants to that of Pre-miR-NC#2 transfectants is shown. *miR-375* significantly suppressed luciferase activity in a target site-dependent manner. The alignment of 2 *miR-375* target sites with mature *miR-375* is also shown. The nucleotide positions in 3′-UTR are indicated. E, negative correlations of *miR-375* and YAP1 expressions in lung cancer cell lines. Left, YAP1 and *miR-375* expressions showed significant negative correlations among the tested lung cancer cell lines. Right, YAP1 was frequently overexpressed in AD and SQ cells, whereas its expression was strongly suppressed in SCLC. In contrast, most SCLC showed overexpression of *miR-375*, whereas *miR-375* was scarcely expressed in the AD and SQ cell lines. F, correlations of ASH1, *miR-375*, and YAP1 expression levels in primary lung cancer specimens. ASH1 and *miR-375* expressions were positively correlated, whereas inverse correlations were present between *miR-375* and YAP1, as well as between ASH1 and YAP1. NL, normal lung; AD, adenocarcinoma; SQ, squamous cell carcinoma; LA, large cell carcinoma; AS, adenosquamous carcinoma.